DOI: 10.1534/genetics.109.112516

A Genomewide RNA Interference Screen for Modifiers of Aggregates Formation by Mutant Huntingtin in Drosophila

Sheng Zhang,*,[1] Richard Binari,*,† Rui Zhou* and Norbert Perrimon*,†,[1]

Department of Genetics and †Howard Hughes Medical Institute, Harvard Medical School, Boston, Massachusetts 02115

Manuscript received November 27, 2009
Accepted for publication January 18, 2010

ABSTRACT

Protein aggregates are a common pathological feature of most neurodegenerative diseases (NDs). Understanding their formation and regulation will help clarify their controversial roles in disease pathogenesis. To date, there have been few systematic studies of aggregates formation in Drosophila, a model organism that has been applied extensively in modeling NDs and screening for toxicity modifiers. We generated transgenic fly lines that express enhanced-GFP-tagged mutant Huntingtin (Htt) fragments with different lengths of polyglutamine (polyQ) tract and showed that these Htt mutants develop protein aggregates in a polyQ-length- and age-dependent manner in Drosophila. To identify central regulators of protein aggregation, we further generated stable Drosophila cell lines expressing these Htt mutants and also established a cell-based quantitative assay that allows automated measurement of aggregates within cells. We then performed a genomewide RNA interference screen for regulators of mutant Htt aggregation and isolated 126 genes involved in diverse cellular processes. Interestingly, although our screen focused only on mutant Htt aggregation, several of the identified candidates were known previously as toxicity modifiers of NDs. Moreover, modulating the *in vivo* activity of *hsp110* (*CG6603*) or *tra1*, two hits from the screen, affects neurodegeneration in a dose-dependent manner in a Drosophila model of Huntington's disease. Thus, other aggregates regulators isolated in our screen may identify additional genes involved in the protein-folding pathway and neurotoxicity.

THE presence of protein aggregates in the brains of patients has long been recognized as a common pathological feature of many neurodegenerative diseases, such as Alzheimer's, Parkinson's, amyotrophic lateral sclerosis (ALS, or Lou Gehrig's disease), and polyglutamine (polyQ) diseases (Rosen *et al.* 1993; Spillantini *et al.* 1997; Sisodia 1998; Gusella and MacDonald 2002; Caughey and Lansbury 2003; Bruijn *et al.* 2004; Ross and Poirier 2005; Pasinelli and Brown 2006). The close link between the diseases and aggregates is especially prominent among polyQ diseases, as best exemplified by Huntington's disease (HD). HD is caused by the expansion of a polyQ tract at the N terminus of the Huntingtin (Htt) protein (Huntington's Disease Collaborative Research Group 1993). In humans, the length of this polyQ tract is normally within the range of 7–26, whereas in HD patients it is invariably expanded to >35 (Andrew *et al.* 1993; Huntington's Disease Collaborative Research Group 1993; Snell *et al.* 1993). One particularly intriguing pathological feature of HD is the presence of intracellular aggregates composed of processed N-terminal Htt (Sisodia 1998; Gusella and MacDonald 2002; Ross and Poirier 2005). The intimate links between aggregates and HD are quite striking. In particular, genetic analyses revealed the existence of an inverse correlation between the length of the polyQ tract and the age of onset of the disease, whereas many *in vivo* and *in vitro* studies have demonstrated that the mutant Htt containing longer glutamine tracts has an increasing propensity to form aggregates (Penney *et al.* 1997; Scherzinger *et al.* 1997). Similar relationships are also observed in eight other polyQ diseases such as spinocerebellar ataxias (Sisodia 1998; Gusella and MacDonald 2002; Ross and Poirier 2005). Because of this intimate link, aggregates have been suspected as the cause of neural toxicity. However, other studies found no correlation between the distribution of aggregates in the brain and neurodegeneration and proposed that aggregates are simply by-products of the disease process. Still other studies have argued that aggregates play a beneficial role by sequestering toxic species within the cell (Sisodia 1998; Gusella and MacDonald 2002; Caughey and Lansbury 2003; Ross and Poirier 2005). Notably, a recent study following aggregates formation in cultured neurons proposed that aggregates formation reduces the levels of diffusive mutant Htt and protects against its toxicity (Arrasate *et al.* 2004).

Supporting information is available online at http://www.genetics.org/cgi/content/full/genetics.109.112516/DC1.

[1]*Corresponding authors:* University of Texas Health Science Center at Houston, SRB–430H, 1825 Pressler St., Houston, TX 77030.
E-mail: sheng.zhang@uth.tmc.edu; and Department of Genetics, Harvard Medical School, 77 Avenue Louis Pasteur, Boston, MA 02115.
Email: perrimon@receptor.med.harvard.edu

Drosophila has been an excellent model system for studying various neurodegenerative diseases (NDs) because toxicity of these disease proteins can often be well recapitulated in the fly (Bilen and Bonini 2005; Marsh and Thompson 2006). Because of this, Drosophila has been widely used to screen for toxicity modifiers of different disease proteins, especially for polyQ diseases, and a diverse group of toxicity modifiers with functions in different cellular processes have been isolated, such as protein folding (*e.g.*, *dnaj1* and *tpr2*) (Chan *et al.* 2000; Kazemi-Esfarjani and Benzer 2000), ubiquitin modification and protein degradation (*e.g.*, *smt3* and *uba2*) (Chan *et al.* 2002; Steffan *et al.* 2004), transcriptional regulation (*e.g.*, *sin3* and *rpd3*) (Fernandez-Funez *et al.* 2000; Steffan *et al.* 2001), and others (Chen *et al.* 2003; Kanuka *et al.* 2003; Shulman and Feany 2003; Ravikumar *et al.* 2004; Wu *et al.* 2005; Cooper *et al.* 2006). Notably, when tested in Drosophila, a human chaperone Hsp70 and a Drosophila co-chaperone *dhdj1* (also known as *Hsp40* or *dnaj1*) can significantly suppress polyQ toxicity and also alter the solubility of aggregates, suggesting a possible correlation between aggregates and neurotoxicity (Warrick *et al.* 1999; Chan *et al.* 2000).

Although Drosophila has been successfully used to identify toxicity modifiers, no comprehensive analysis of regulators of aggregates formation has been conducted, probably due to a lack of a simpler assay to assess the aggregates formed *in vivo*. To systematically identify central regulators of protein aggregation in this model organism, we focused on the well-studied HD protein Htt. Earlier studies in different model systems have already demonstrated that expression of mutant Htt or other polyQ disease proteins induces polyQ-length-dependent neurodegeneration (Gusella and MacDonald 2002; Bilen and Bonini 2005; Marsh and Thompson 2006). To evaluate the aggregates formation by mutated Htt in Drosophila, we first generated transformant lines for enhanced GFP (eGFP)-tagged Htt exon 1 fragments containing different lengths of glutamine repeats and analyzed their ability to form aggregates in Drosophila tissues. We then established a cell-based quantitative assay that allows automated measurement of aggregates within cells by combining automated microscopy with quantitative analysis. Using this automated protocol, we performed a high-throughput genomewide RNA interference (RNAi) screen in Drosophila cells and identified a diverse group of genes that can affect formation of aggregates by mutant Htt.

MATERIAL AND METHODS

DNA plasmids: DNA containing the mutant Httex1-Qn-eGFP variants (Q25, Q46, Q72, and Q103) were generously provided by the Hereditary Disease Foundation [originally from A. Kazantsev (Kazantsev *et al.* 1999)] and cloned into the hygromycin-resistance pMK33 vector that contains the copper-inducible *metallothionein* promoter. See File S1 for details about the plasmids and cloning procedures.

RNAi screen: Using a MultiDrop liquid dispenser, stable Httexon1-Qp47-eGFP cells were aliquoted uniformly into 384-well double-stranded RNA (dsRNA)-containing plates at ~1×10^4 pMK33-Httex1-Qp46eGFP cells per well in 20 μl of serum-free medium. After incubation at room temperature for 1 hr, 20 μl of medium containing 10% fetal bovine serum (FBS; JRH Biosciences) was added. After 3 days of incubation, 25 μl of medium containing $CuSO_4$ and 5% FBS was added to each well to reach a final copper concentration of 400 μM to induce the expression of the Httex1-Qp46-eGFP reporter. After induction for another 2 days, cells were fixed using 4% formaldehyde at room temperature for 20 min. For cell staining, the samples were washed three times with PBST (1× PBS plus 0.1% Triton-X100) after fixation and then incubated with DAPI (0.2 μg/ml final concentration; Molecular Probe) and TRITC-conjugated phalloidin (10 ng/ml final; Sigma) in PBST for 30 min to label nuclei and F-actin, respectively, followed by washing four more times with 1× PBST.

Image acquisition and data analysis: Using the ×20 objectives on an automated Nikon TE300 microscope, triple-channel images from four different sites in each well were captured: the FITC channel for the level of eGFP expression and information on aggregates within the site; the DAPI channel for cell nuclei; and the TRITC channel for overall cell morphology. Images from the FITC and DAPI channels in each site were quantified using MetaMorph software (Universal Imaging) to calculate the number, size, and signal intensity of the aggregates and determine the cell number within the site. For aggregates, images from the FITC channel were segmented on the basis of a predetermined threshold parameter and their fluorescent intensity was calculated; because the aggregates are highly enriched with the eGFP-tagged mutant Htt (Httex1-Qp46-eGFP), the level of fluorescent signal from the aggregates is significantly higher than that from the cytoplasm and from background noise, thus allowing their clear identification and quantization by the software (see Figure 2B). To ensure the accuracy of this automated quantization, we also performed visual scoring and manual quantization for a few selected sites in each plate and confirmed that the manual results were comparable to those from the automated quantization. Similarly, cell numbers in the same site were counted by analyzing the corresponding DAPI channel images. In general, ~4000 cells were analyzed for every dsRNA-treated sample. The information on aggregates and cell number was then used to calculate the three parameters for evaluating the effect of dsRNA treatment on aggregates formation: the average number, size, and signal intensity of the aggregates, which were further normalized with the cell number in each site. Results from all four sites in the same well were then averaged to access the aggregation status in this dsRNA-treated well.

Primary screens: Two sets of 63 plates from the Drosophila RNAi Screening Center and three sets of two kinase/phosphatase plates from M. Kulkarni (M. M. Kulkarni and N. Perrimon, personal communication), containing 250 ng of dsRNA per well, were screened. For each plate screened, the average value and standard deviation (SD) on these three evaluation parameters from the whole plate were also calculated. In the primary screen, those dsRNAs that decreased or increased the aggregates formation by >2× SD from the whole-plate average for any of the three evaluation parameters were considered to have a significant effect on aggregates formation and were selected as potential candidates. See File S1 for detailed description of assays in secondary screens.

Drosophila stocks: The Httex1p-Q93 and Q48-myc/Flag flies were generously provided by L. Thompson and J. L.

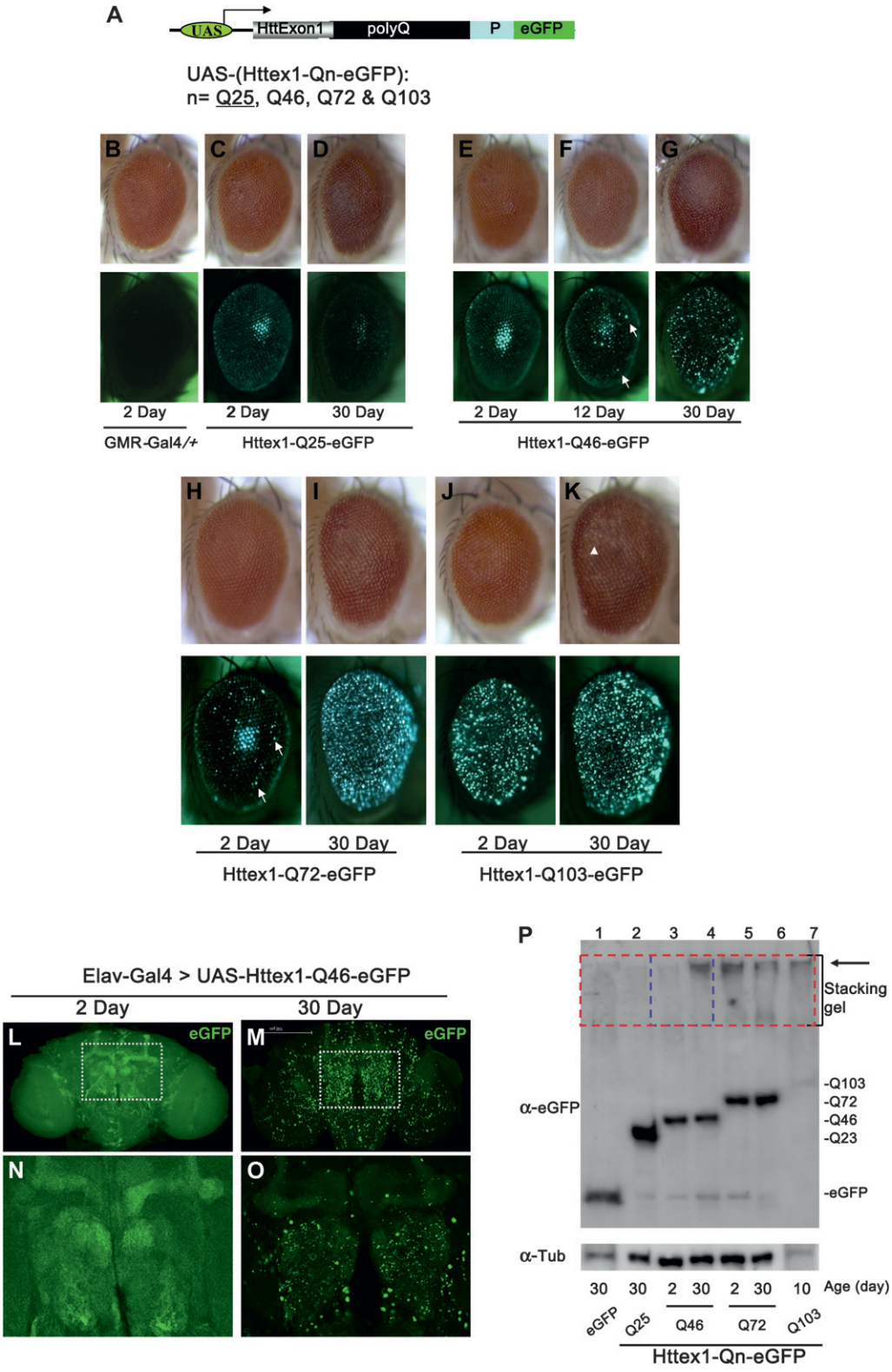

FIGURE 1.—Age- and polyQ-length-dependent formation of aggregates in Drosophila. (A) Structure of the Htt exon1 (Httex1) constructs used for the studies. eGFP-tagged Httex1 with different lengths of glutamine tract (polyQ) followed by its proline-rich region (P) are under the control of the UAS elements (BRAND and PERRIMON 1993). (B–P) PolyQ-length- and age-dependent formation of aggregates in Drosophila. (B–K) Httex1-Qn-eGFP were expressed in the eye using the eye-specific *GMR*-Gal4 driver. (Top) The general eye morphology of adults of different ages. (Bottom) Images of the same eyes under green fluorescent light, with their age and genotype indicated below. Genotypes: (B) *GMR*-Gal4/+ and (C–K) *GMR*-Gal4/+; *UAS*-Httex1-Qn-eGFP/+. (B) Control of *GMR*-Gal4 driver alone at day 2. Note that there is no visible eGFP signal in this eye (bottom) in the absence of the *UAS*-eGFP reporter. (C and D) Adult eyes with Httex1-Q25-eGFP expression. Q25 is found mainly in a diffuse cytoplasmic pattern at both day 2 (C) and day 30 (D). Note that the center bright spots in both eyes and in E are not aggregates but rather an optical phenomenon similar to the "deep pseudopupil," arising from the superimposition of evenly diffuse GFP signals emitted from the underlying regularly arranged ommatidia (FRANCESCHINI 1972). (E–G) Adult eyes with Httex1-Q46-eGFP expression. At day 2 (E, left eye), Httex1-Q46 is found mainly in a diffuse cytoplasmic pattern. As the fly ages, sporadic aggregates gradually accumulate (F, white arrows) and become prominent by day 30 (G). (H and I) Adult eyes with Httex1-Q72-eGFP expression. At day 2 (H), Q72 is found mainly in a diffuse cytoplasmic pattern but sporadic aggregates are already visible (H, white arrows). Aggregates become prominent by day 30 (I). (J and K) Adult eyes with Httex1-Q103-eGFP expression. Aggregates already become prominent at day 2 (J) and persist at day 30 (K). Note also that there is a mild loss of pigment at the posterior of this eye at day 30 (K, white arrowhead), indicating the degeneration of underlying eye tissues at this stage. In all images, the eyes are oriented as dorsal side is up and anterior is to the right. (L–O) Confocal images of aggregates formation in the brain by the Httex1-Q46-eGFP, which was expressed in the CNS using the pan-neuronal *Elav*-Gal4 driver. Genotypes: *Elav*-Gal4/+; *UAS*-Httex1-Q46-eGFP/+. The protein was distributed evenly, and no obvious aggregates were found in the brain at the younger age (L and N, day 2), whereas

Marsh (Steffan *et al.* 2001). The genotype of HD93 flies in the genetic testing is *GMR*-Gal4/+; *UAS*-Httex1p-Q93. The following fly *hsp110* alleles showed dosage-dependent genetic interaction with the HD93 flies: *l(3)00082*, *l(3)S031820*, *l(3)S064906*, *l(3)S004112*, and *l(3)S0134802*. The following *tra1* alleles were tested and showed dosage-dependent genetic interaction with the HD93 flies *Nipped-A*^{NC116} and *Nipped-A*^{NC186}. See File S1 for a detailed description of genetic crosses and fly stocks. Additional information can be found in File S1.

RESULTS

Htt mutants form aggregates in a polyQ-length- and age-dependent manner in Drosophila tissues: To screen for regulators of aggregates formation, we first needed to select a mutant disease protein whose propensity to form aggregates could be modulated by the cellular genetic environment. Htt mutants are ideal candidates for this purpose, given the unique feature of a correlation between their propensity to form aggregates and the length of their polyQ tracts (Scherzinger *et al.* 1997; Gusella and MacDonald 2002). Accordingly, we focused our study on the well-established Htt exon 1 (Httex1) constructs, which contain different lengths of the polyQ tract: Httex1 with 25 glutamines (Q25) representing wild-type Htt control and mutated Htt containing an increasing length of the glutamine repeats 46Q, 72Q, and 103Q (simplified from here on as Httex1-Q25, -Q46, -Q72, and -Q103) (Kazantsev *et al.* 1999). These Httex 1 proteins, which are tagged at their C termini with eGFP, have been previously shown to form visible polyQ length-dependent aggregates in cultured mammalian cells (Kazantsev *et al.* 1999). We cloned this set of eGFP–Httex1 constructs into the pUAST vector and generated corresponding transgenic fly lines, which allow the targeted expression of Httex1 transgenes in selected tissues using the Gal4 binary expression system (Figure 1A) (Brand and Perrimon 1993).

We then examined the aggregation property of these Httex1 proteins in several Drosophila tissues. Remarkably, when expressed in the eye using the eye-specific GMR-Gal4 driver, the aggregation patterns of the eGFP-tagged Httex1 proteins can be conveniently monitored directly in adult fly eyes under fluorescence microscopy (Figure 1, B–K). For example, while Httex1-Q25 maintains a diffuse cytoplasmic distribution over the life of the fly (Figure 1, C and D), Httex1-Q103 exists almost exclusively in prominent aggregates soon after it is expressed and is already prominent in newly hatched adults (Figure 1, J and K, and data not shown). Furthermore, while the expression of both Httex1-Q46 and -Q72 is diffuse in young flies, aggregates gradually develop as the flies age, with Q72 forming aggregates at a faster rate than Q46 (Figure 1, E–I).

We next analyzed aggregates formation by these Httex1 proteins in the fly central nervous system (CNS). When expressed in all neuronal cells using the pan-neuronal Elav-Gal4 driver, these Httex1 proteins showed aggregation patterns similar to those in the eye (Figure1, L–O, and data not shown). Notably, again among the tested Httex1 proteins, the age-dependent nature of aggregates formation was most clearly exemplified in flies expressing Httex1-Q46. As shown by confocal imaging in 2-day-old adult flies, Httex1-Q46-eGFP protein was evenly distributed in the brain (Figure1, L and N). However, by day 30, predominant eGFP-positive aggregates were present throughout the brain (Figure1, M and O). Thus, consistent with the observations in mammalian cells, these Htt exon1 proteins show both age- and polyQ-length-dependent patterns of aggregates formation in Drosophila tissues.

An important biochemical definition of protein aggregates is their resistance to detergent SDS, which can be detected on Western blot as SDS-insoluble large protein complexes that are retained in the stacking gel. To confirm that the observed bright eGFP-positive puncta in Drosophila tissues are indeed protein aggregates, we extracted whole proteins from adult fly heads at different ages and performed Western analysis. As shown in Figure 1P, SDS-resistant large protein complexes were absent in 30-day-old control flies expressing eGFP alone or eGFP-tagged wild-type Httex1-Q25; they were present in both young (2-day-old) and aged (30-day-old) Httex1-Q72 and Httex1-Q103 flies; most tellingly, these complexes were absent in young flies (2-day-old) but were clearly present in aged (30-day-old) Httex1-Q46 flies (lanes 3 and 4 in Figure 1P, highlighted with blue dashed lines), mirroring the appearance of eGFP-positive puncta in these animals. Thus, the development of SDS-insoluble large protein complexes, a process that is also both polyQ length and age dependent, correlates with the appearance of eGFP-positive puncta in the fly tissues, indicating that these fluorescent puncta are indeed protein aggregates.

In addition to aggregates formation, we also observed the expected, polyQ-length-dependent toxic effect of

numerous prominent aggregates were present at day 30 (M and O). (N and O) Higher magnification view of regions (the olfactory bulb and the α- and β-lobes of mushroom body) highlighted in L and M, respectively. Note that the images in the younger brain (L and N) were exposed for a longer time to maximize the detection for aggregates. (P) Confirmation by Western blot of the development of SDS-insoluble aggregates in Httex1-Qn-eGFP flies. Whole-protein extracts from adult fly heads were probed with anti-eGFP antibody. (Bottom) Ages and the type of the expressed protein in the examined flies. Large protein complexes that were retained in the stacking gel, as highlighted, were found in samples from Httex1-Q72, Q103 (lanes 5–7) and aged Q46 flies (lane 4, 30 days old), but were absent in young Q46 flies (lane 3, 2 days old) and other control flies (lane 1, flies expressing eGFP alone; lane 2, Httex1-Q23-eGFP; both were 30 days old).

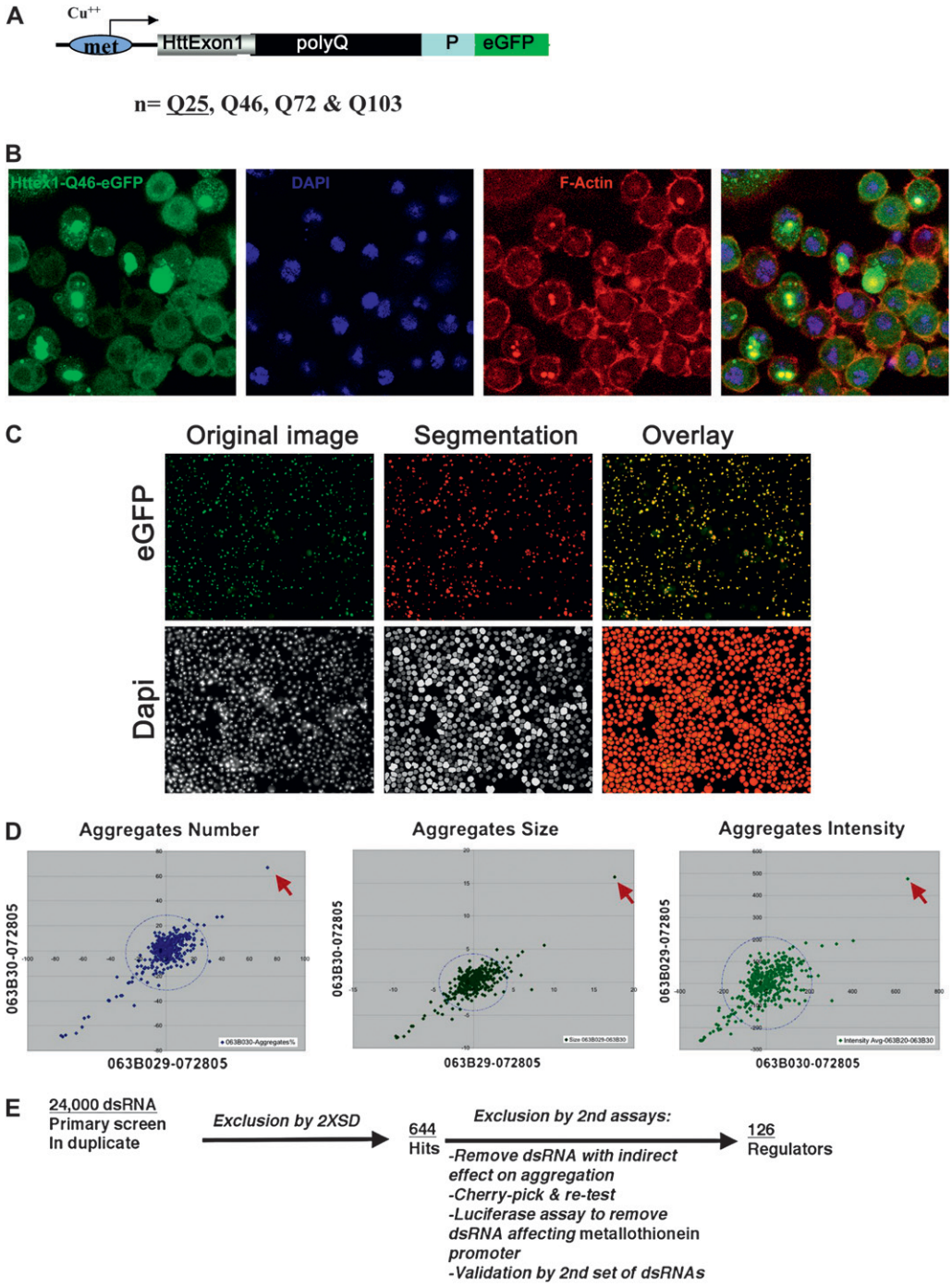

FIGURE 2.—Imaging-based high-throughput genomewide RNAi screen for modifiers of aggregates formation in Drosophila cells. (A) Structure of the Httex1-eGFP reporter construct used in the cell-based assay, which is under the control of the copper-inducible (Cu^{++}) *metallothionein* (met) promoter. (B) Confocal images of aggregates formation by Httex1-Qp46-eGFP in Drosophila S2 cells. Note that only ~50% of the cells developed prominent aggregates, whereas in the remaining cells the Httex1-Qp46 protein was present diffusively in the cytoplasm. Aggregates were identified by the prominent eGFP signals (green), overall cell morphology using the TRITC-labeled phalloidin stain (red), and cell nuclei stained by DAPI (blue). (C) Automated quantification of aggregates and cell number. Aggregates were revealed by their prominent eGFP signals and the cell nuclei by DAPI staining (left). Overlaying of computer-simulated objects on the basis of quantification analyses (middle) with their original images revealed significant overlap, demonstrating the accuracy of this quantification method (right). (D) Scattered plot comparison of quantification results for two duplicate plates based on the parameters of average aggregates number (left), size (middle), and intensity (right). The circular dashed lines indicate a radius of 2× SD for each parameter. Most dsRNAs tested are within the 2× SD range, with the position of CG6603 highlighted (red arrows). (E) Flow chart for the genomewide RNAi screen to isolate modifiers of aggregates formation.

these mutant Httex1 proteins; that is, Httex1 with longer polyQ tracts causes more severe degenerative phenotypes, such as reduced survival rate during development, as well as progressive eye degeneration, declining mobility, and shortened life span in adults (arrowhead in Figure 1K and data not shown). Together, these results demonstrated that both the formation of aggregates and the toxicity of mutant Htt could be recapitulated in Drosophila expressing eGFP-tagged Htt-exon1-Qn reporters. Furthermore, among the tested Httex1 proteins, the progressive nature of aggregates development was most clearly exhibited by Httex1-Q46-expressing animals, suggesting that Httex1 with an intermediate length of glutamine repeats (*i.e.*, Q46) might be more susceptible to modulations by other cellular factors and thus represents a good candidate as a reporter in screens for regulators of aggregates formation.

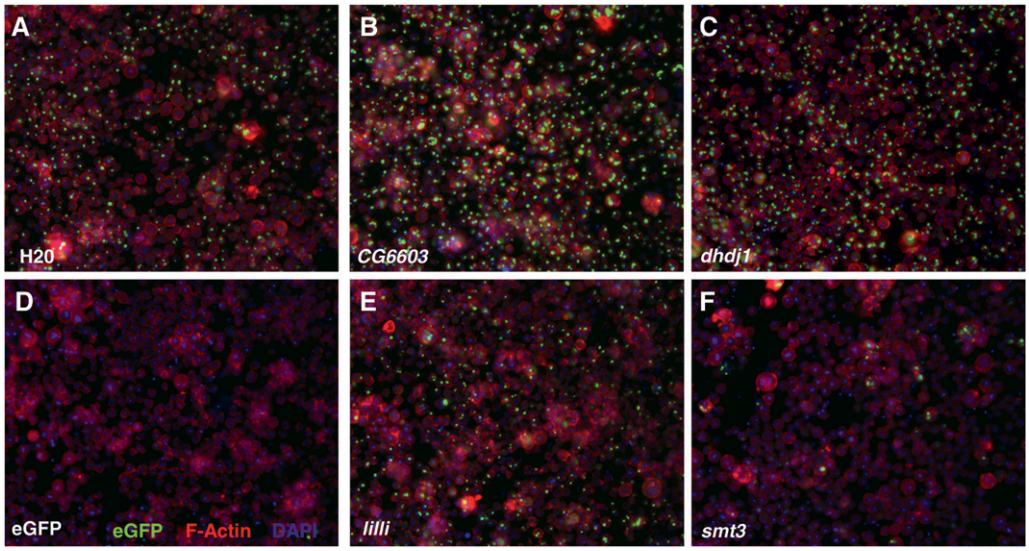

FIGURE 3.—Sample images from the RNAi screen. Examples of images from wells treated with a water control (A) or dsRNAs against eGFP (D), *CG6603* (B, *dhsp110*), *dhdj1* (also known as *dnaj1* or *hsp40*) (C), *lilli* (E), and *smt3* (F). Aggregates were identified by the prominent eGFP signals (green), overall cell morphology using the TRITC-labeled phalloidin stain (red), and cell nuclei stained by DAPI (blue).

An imaging-based, high-throughput assay for aggregates formation in Drosophila cells: With the recent advent of RNAi technology and the development of genomewide dsRNA libraries, it is possible to quickly and systematically evaluate all known genes in a model organism for their effects on a studied question. In Drosophila, RNAi-mediated gene knockdown is especially efficient in cultured cells, and genomewide RNAi screens have been well developed and applied to exploring multiple signaling (CAPLEN *et al.* 2000; CLEMENS *et al.* 2000; FRIEDMAN and PERRIMON 2007). To establish a relevant cell-based assay suitable for an RNAi screen for aggregation regulators in Drosophila, we chose hemocyte-like S2 and neuronal-like BG2 cells and generated stably transformed cell lines in which the expression of the above eGFP-tagged Httex1 proteins is controlled by the copper-inducible *metallothionein* promoter (Figure 2A). Consistent with the *in vivo* results in both of these two cell lines, these Httex1 proteins showed behavior similar to polyQ-length-dependent aggregation (Figure 2B and data not shown). Importantly, aggregates in these cells emit intense fluorescent signals that are easily identifiable even when viewed at low magnification (Figure 2C), making it feasible to use the image-based approach to screen for aggregates regulators.

In adopting such an image-based assay for a high-throughput screen, it is important that individual aggregates and each cell can be clearly distinguished to ensure reliable quantification. We found that, under the cultured condition, neuronal-like BG2 cells more easily congregate together and form clumps even before reaching confluence, impeding the clear visualization and quantification of both the aggregates and cell number (data not shown), while such issues are much less prominent in S2 cells, which are more prone to spread out and form a single layer over the surface before reaching confluence (Figure 2B). Moreover, in the established S2 cell line expressing Httex1-Q46-eGFP, aggregates develop in ~50% of the cells, which is ideal for a modifier screen to identify both suppressors and enhancers of mutant Htt aggregation (Figure 2B). Accordingly, we chose this S2 cell line expressing Httex1-Q46-eGFP for the ensuing RNAi screen.

To demonstrate the relevance and sensitivity of this cell-based system for a modifier screen, we treated these cells with a dsRNA against *dhdj1*, a known suppressor of aggregates (CHAN *et al.* 2000; KAZEMI-ESFARJANI and BENZER 2000), and found that it significantly enhanced aggregates formation (Figure 3C); conversely, treatment with dsRNA targeting the eGFP tag in the Httex1-Q46 reporter completely abolished fluorescent signals (Figure 3D).

To ensure that this cell-based assay could be applied to a high-throughput screen, we further developed an automated assay protocol. Using this protocol, sample images were captured by an automated microscope, with aggregates revealed by their prominent eGFP signals and individual cells by DAPI nuclear staining. Details about the aggregates (*i.e.*, the size, total number, and signal intensity of aggregates) and the number of cells in the imaged fields were automatically quantified using the MetaMorph analytic software. Since the aggregates are highly enriched with eGFP-tagged mutant Htt (Httex1-Q46-eGFP), the level of fluorescent signal from the aggregates is significantly higher than that from the cytoplasm and from background noise, thus allowing their clear identification and quantification. As seen in Figure 2C, this automated quantification gave rise to satisfactory accuracy in measuring both the aggregates and the cell number (see legend for Figure 2C and MATERIALS AND METHODS for details).

When evaluated by such a quantitative approach, most dsRNAs tested show no effect on aggregates formation, while dsRNA specifically directed against *dhdj1* as a positive control significantly enhanced aggregates for-

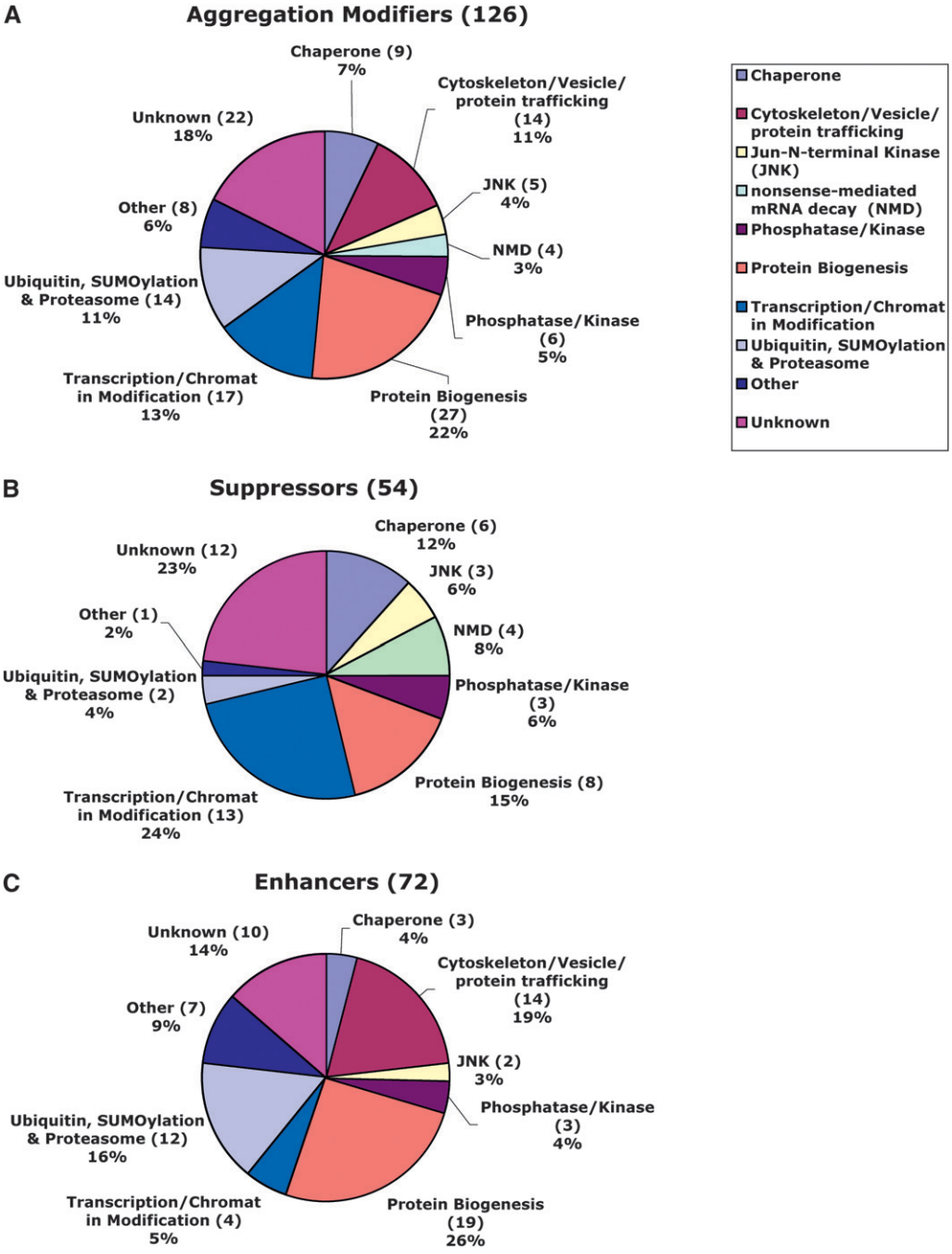

FIGURE 4.—Functional categorization of aggregation regulators from the screen. Pie chart representation of candidate genes based upon their Gene Ontology index biological function or protein domains shows the categories of all 126 hits (A) and the 54 suppressors (B) and 72 enhancers (C) that can modulate the formation of mutant Htt aggregates from the screen. "Enhancer" is defined genetically as the gene that causes reduced aggregates formation after RNAi-mediated knockdown of target gene expression in the assay. Conversely, "suppressor" is defined as the gene that causes increased aggregates formation when its expression is knocked down.

mation, and *dhdj1* was reproducibly categorized as a strong suppressor (Figure 3C). Furthermore, comparison between duplicate experiments reveals that overall both the assay and the quantification results are highly reproducible (Figure 2D and data not shown).

Genomewide RNAi screens for regulators of aggregates formation: *Primary screens:* After optimization of this cell-based assay in a 384-well plate format, we performed an RNAi screen in duplicate using a Drosophila genomewide library of ~24,000 dsRNAs (BOUTROS *et al.* 2004), with the effect of each dsRNA on aggregates formation quantified on the basis of three parameters: the average number, size, and signal intensity of aggregates (Figure 2D, and supporting information, Figure S1). For each plate, the average value and SD for these three parameters from whole-plate samples were also calculated. For a dsRNA-treated sample in the primary screen, if the value of any of the three parameters was $>2 \times$ SD of the whole-plate average, it was considered to have a significant effect on aggregates formation and was selected as a potential candidate (Figure 2, D and E; also see MATERIALS AND METHODS for screen details). On the basis of the above selection criterion, we identified 644 candidate dsRNAs from the primary screens that potentially enhance or suppress aggregates formation.

TABLE 1

Aggregation modulators isolated from the screen

Functional classes	No. of modulators	Suppressors	Enhancers
Chaperone	9	6	3
Cytoskeleton/vesicle/protein trafficking	14	—	14
Jun-N-terminal kinase	5	3	2
Nonsense-mediated mRNA decay	4	4	—
Phosphatase/kinase	6	3	3
Protein biogenesis	27	8	19
Transcription/chromatin modification	17	13	4
Ubiquitin, SUMOylation and proteasome	14	2	12
Other	8	1	7
Unknown	22	12	10
Total	126	52	74

Table 1 lists the functional classes for the aggregation modulators isolated from the screen (column 1), the total number of modifiers in each functional class (column 2), as well as the number of modifiers in each enhancer and suppressor subset (columns 3 and 4). Candidates were categorized on the basis of the Gene Ontology biological function or protein domains. "Suppressor" is defined genetically as those candidates that cause an increased formation of aggregates after dsRNA-mediated knockdown of the corresponding candidate gene, and vice versa. "Enhancer" is similarly defined as those candidates that cause a decreased formation of aggregates in the assay (also see Figure 3 and Table S1 and Table S2 for more details).

Secondary assays: To eliminate false positives resulting from indirect effects on aggregates formation, we further evaluated the 644 candidate dsRNAs from the primary screen in the following steps (Figure 2E and Figure S2; see legends and MATERIALS AND METHODS for details): (1) removed dsRNA amplicons that contain 21-bp overlaps with more than 5 other genes in the genome, which are expected to cause significant nonspecific off-target RNAi effects (KULKARNI *et al.* 2006; MA *et al.* 2006); (2) removed dsRNA amplicons that are known to function in general protein synthesis (*e.g.*, cytoplasmic or mitochondrial ribosomal proteins), which affects overall protein synthesis within the cell, indirectly affecting the formation of aggregates that depends upon the amount of available misfolded Htt protein (SCHERZINGER *et al.* 1999); (3) removed dsRNA amplicons that failed to reproduce their effect on aggregation in an intermediate screen using the resynthesized dsRNAs; (4) identified and removed candidates that affect the activity of *metallothionein* promoter in a luciferase-based assay (*e.g.*, COPI coatomer complex components and the copper transporter); (5) validated each remaining hit by synthesizing and retesting one or two more dsRNAs targeting different regions of the candidate gene. Genes that failed to repeat their effect on modulating aggregation in these additional rounds of testing were removed from consideration. In total, 126 genes passed both the primary screens and all subsequent validation steps (Figure 2E and Figure S2).

Functional categorization of regulators of aggregates formation identified by the screen: Of the 126 validated regulators from the screen, 52 act as enhancers and 74 as suppressors of aggregates formation (Figure 4, A–C, and Table 1; see Table S1 and Table S2 for a list of these genes and associated information). Throughout this study, "suppressor" is defined genetically as a candidate that causes an increased formation of aggregates after dsRNA-mediated knockdown of the corresponding gene. And vice versa, "enhancer" is similarly defined as a candidate that leads to a decreased formation of aggregates in the assay. Examples of some of these modifiers are shown in Figure 3. Interestingly, although overall only 50% of fly genes are conserved in humans (RUBIN *et al.* 2000), 71% (90 of 126) of isolated candidates have predicted human orthologs, with 25 of them encoding proteins that have been implicated in human diseases (see Table S2).

On the basis of their predicted function, these 126 genes can be further categorized into different classes, the largest category of which contains genes that function mainly in protein biogenesis (Figure 4A and Table 1). Interestingly, the major classes of suppressors from a *Caenorhabditis elegans* screen in the muscle tissue for modifiers of polyQ aggregation are also involved in protein biogenesis, which has been proposed to represent the "protein homeostatic buffer" that can respond to and prevent the aggregation of misfolded proteins (NOLLEN *et al.* 2004; MORIMOTO 2008).

In addition, all 14 genes in the cytoskeleton/protein trafficking group were isolated as enhancers of aggregation, suggesting that formation of visible aggregates might involve active transport to concentrate misfolded proteins into a specific compartment within the cell (GARCIA-MATA *et al.* 1999), while interference with cytoskeleton integrity or the protein transport machinery might disrupt such a process.

In eukaryotes, multiple families of chaperones with diverse cellular functions are present (CRAIG *et al.* 1994; WHITESELL and LINDQUIST 2005; BUKAU *et al.* 2006). Within the cell, chaperones are essential in facilitating

TABLE 2

Aggregation regulators previously identified as toxicity modifiers

Modifier name	Function	Modification of NDs	Reference
14-3-3ε	Adaptor protein	PolyQ (SCA1)	Chen *et al.* (2003)
MADM	Adaptor protein	PolyQ	Wu *et al.* (2005)
DnaJ-1	Chaperone (Hsp40)	PolyQ (SCA3)	Chan *et al.* (2000); Kazemi-Esfarjani and Benzer (2000)
Hsc70-4	Chaperone	PolyQ (SCA3)	Chan *et al.* (2000); Warrick *et al.* (2000)
CG6603	Chaperone Hsp110	PolyQ (HD)	This study
Rpd3	Chromatin modification/transcription	PolyQ (SCA1)	Fernandez-Funez *et al.* (2000)
Sin3A	Chromatin modification/transcription	PolyQ (HD)	Steffan *et al.* (2001)
Atxain-2	Cytoskeleton	PolyQ (SCA1) and AD (Tau)	Shulman *et al.* (2003)
Smt3	SUMO modification	PolyQ (HD)	Steffan *et al.* (2004)
Uba2	SUMO modification	PolyQ (SBMA)	Chan *et al.* (2002)
Tra1 (*Nipped-A*)	Kinase/transcriptional regulation	PolyQ (HD)	This study
Tor	TOR signaling/autophagy	PolyQ (HD)	Ravikumar *et al.* (2004)
Sec61α	Translocon/protein trafficking	PolyQ (HD)	Kanuka *et al.* (2003)
Nup44A[a]	Nuclear pore component/protein trafficking	PolyQ (SCA1)	Fernandez-Funez *et al.* (2000)
Pros26[a]	Proteasome	PolyQ (SCA1)	Fernandez-Funez *et al.* (2000)
Rab1	Vesicle/protein trafficking	PD (α-synuclein)	Cooper *et al.* 2006
Tao-1	STE20-related kinase/JNK	AD (Tau)	Shulman *et al.* 2003

Table 2 lists the known toxicity modifiers of neurodegenerative diseases (NDs) that were also isolated as modifiers of aggregates formation from the RNAi screen. PolyQ, polyglutamine diseases; HD, Huntington's disease; PD, Parkinson's disease; AD, Alzheimer's disease; SCA, spinocerebellar ataxia type; SBMA, spinalbulbar muscular atrophy.

[a] Pros26 and Nup44A were not themselves isolated as modifiers of aggregation, but several other components in either the proteasome complex or the nuclear pore complex were isolated in the screen.

the proper folding of newly synthesized proteins and the refolding of misfolded proteins to maintain them in their soluble native state (Craig *et al.* 1994; Whitesell and Lindquist 2005; Bukau *et al.* 2006). Since the aggregates in this assay were derived from misfolded mutant Htt, it is expected that chaperones play a central role in regulating aggregates formation. Indeed, another major class of modifiers from the screen includes several chaperones and their regulatory proteins, such as the chaperone proteins *CG6603* (a member of Hsp110 subfamily chaperones; see below), *hsp83* (Hsp90 family), and *hsc70-5* (Hsp70 family); the co-chaperone *dhdj1* (Hsp40 family); chaperonin *T-cp1*; and the heat-shock transcription factor *hsf*. *Hsf* is activated in response to heat shock and other cellular stresses to induce the expression of downstream chaperone proteins (Craig *et al.* 1994). Knockdown of all these chaperone genes enhanced aggregates formation (*i.e.*, suppressors), while depletion of *CG6603* gave rise to the strongest enhancing effect of all the regulators isolated (Figure 2D and Figure 3B; also see below). Surprisingly, knockdown of both *hsc70-3* and *hsc70-4*, two abundant Hsp70 chaperones, caused reduction of aggregates formation. Previous studies suggest that each chaperone has selective substrate preferences, and chaperones further show specificity in modulating polyQ neurotoxicity (Chan *et al.* 2000). In addition, some chaperones are known to be involved in essential cellular processes. For example, *hsc70-4* in Drosophila is critical for clathrin-dependent endocytosis (Chang *et al.* 2002, 2004). Thus, modulating the activities of these chaperones might indirectly affect the aggregates formation, and their observed differential effect on aggregation could be due to their distinctive cellular functions and substrate specificity. Moreover, a dozen modifiers, such as *uba1*, *smt3*, and *lwr*, are involved in ubiquitin- or sumo-modification and protein degradation pathways, indicating that clearance of misfolded proteins by the cellular degradation machinery serves as an important regulatory step in aggregates formation.

Notably, several components of the nonsense-mediated mRNA decay (NMD) pathway were isolated, which all acted as suppressors of aggregates formation. NMD is a cellular surveillance machinery that promotes the degradation of abnormal mRNAs containing premature termination codons (Valencia-Sanchez and Maquat 2004). The potential mechanism for the NMD pathway in modulating aggregation formation is not clear. Interestingly, one central component of the NMD complex, *smg1*, encodes a large protein with a PI3,4-kinase domain, a Huntingtin, elongation factor 3, protein phosphatase 2A, and the yeast PI3-kinase TOR1 (HEAT) repeat domain, and, notably, a heat-shock protein Hsp70-like domain (Gatfield *et al.* 2003). This raises the possibility that the NMD pathway also has some functional overlap with the chaperone machinery and, as such, senses and modulates the formation of aggregates through its crosstalk with chaperones. Alter-

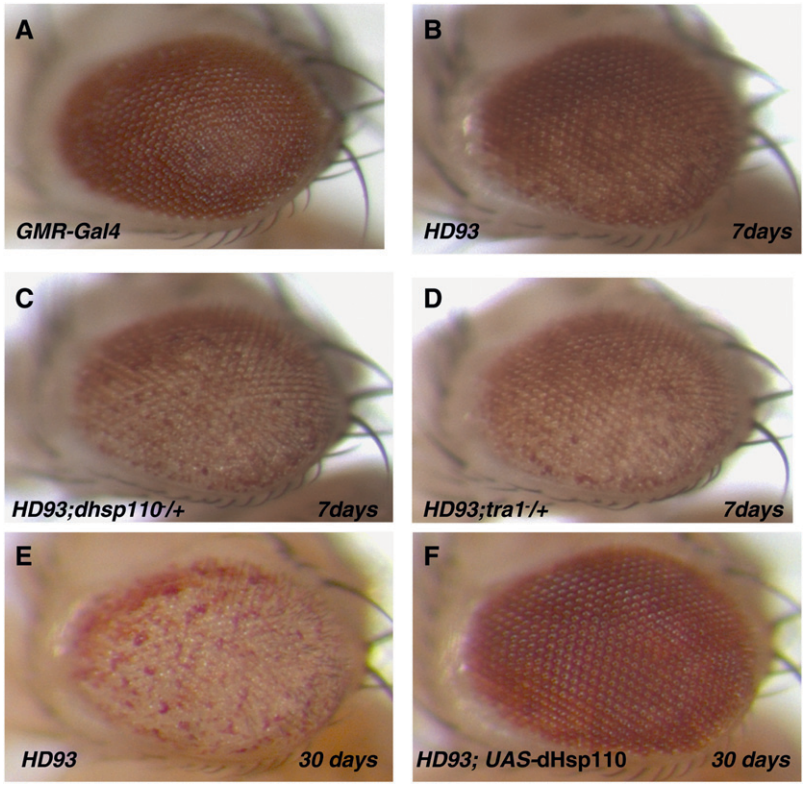

FIGURE 5.—*In vivo* modification of the neurodegeneration phenotype associated with a Drosophila HD model by Hsp110 and Tra1. In 7-day-old HD93 flies (genotype: *GMR*-Gal4/+; *UAS*-Httex1p Q93/+) (STEFFAN *et al.* 2001), degeneration is manifested externally by the loss of pigmentation in the posterior of the eye (B), as compared to the control of *GMR*-Gal4 eyes (A). By day 30, the degeneration has expanded to encompass the entire eye (E). In a heterozygous *hsp110* (*dhsp110*) mutant background, the degeneration was accelerated and had spread to the entire eye by day 7 (C). Such degeneration was significantly suppressed by coexpression of wild-type Drosophila Hsp110 (dHsp110), even at day 30 (F). See also Figure S4 for additional controls for the test. The eye degeneration phenotype of HD93 flies was also significantly accelerated in a heterozygous *tra1* mutant background (D). In all eye images, the anterior side is up and the ventral side is to the left.

natively, since NMD acts by promoting the decay of abnormal mRNAs, another attractive possibility is that it recognizes the expanded CAG repeats in the mRNA transcripts of mutant Htt and promotes their degradation (VALENCIA-SANCHEZ and MAQUAT 2004).

A number of kinases and phosphatases were also isolated from the screen, including a PI-3,4 kinase PI3K68D, the α- and β-subunits of casein kinase II (CKII), as well as the phosphatases *CG1906* and *spaghetti*. *CG1906* encodes a phosphatase 2C-like protein, while *spaghetti* encodes a tetratricopeptide repeat (TPR)-containing protein with serine/threonine phosphatase activity. The exact role of these signaling molecules in modulating aggregates formation remains to be clarified. Notably, *spaghetti* was reported to interact with chaperone Hsp90, another aggregates regulator isolated from the screen, and normally forms a large chaperone complex (MARHOLD *et al.* 2000). This raises the possibility that *spaghetti* affects aggregates formation by regulating the activity of chaperones within the cell. It is not clear if these kinases and phosphatases function together and converge on the same pathway (such as the chaperones) or exert their effect through separate pathways. Because kinases and phosphatases provide targets of choice in drug design, it will be of interest to identify the exact pathway(s) regulated by these signaling molecules to decipher how they influence aggregates formation.

Another potential class of modifiers, including *jra1*, *raw*, *tao1*, *cka*, and *lic*, is involved in Jun-N-terminal kinase (JNK) signaling. The presence of aggregates within the cell might trigger a cellular stress/defense response, which is normally mediated by the JNK-signaling pathway (WESTON and DAVIS 2002).

We also noted that, although our screen focused on identifying regulators of aggregates formation, a number of isolated candidates from the screen have been previously identified as toxicity modifiers for polyQ or other aggregates-associated diseases (Table 2). For example, *smt3* and *uba* 2, which encode SUMO protein and SUMO-activating enzyme, respectively, have been shown previously to modulate polyQ pathogenesis in Drosophila (CHAN *et al.* 2002; STEFFAN *et al.* 2004), and both were isolated in our screen as aggregation enhancers. Similarly, *sin3A* and *rpd3*, which are components of the Sin3 chromatin-remodeling complex involved in transcriptional repression and were previously characterized as modifiers of polyQ toxicity (FERNANDEZ-FUNEZ *et al.* 2000; STEFFAN *et al.* 2001), were identified in our screen as aggregation suppressors. In addition, *tao1* has been reported to be involved in tauopathy and *rab1* to be associated with α-synuclein-induced toxicity (SHULMAN and FEANY 2003; COOPER *et al.* 2006). It is possible that the mechanisms by which these genes modulate neurodegeneration are completely separable from their role in regulating aggregates formation. For example, it has been suggested that through the SUMO modification of Htt, *smt3* and *uba2* might modulate cellular toxicity by affecting Htt's transcriptional repression activity or its subcellular localization (CHAN *et al.* 2002; STEFFAN *et al.* 2004). Nevertheless, the observation of an overlap between these two groups of modifiers raises the possibility that the effects of these modifiers on aggregates

formation also contribute to their role in modulating neuronal toxicity.

Hsp110 as a potent suppressor of aggregates formation and neurotoxicity: CG6603 was isolated as the most potent aggregates suppressor from the screen: RNAi-mediated depletion of CG6603 caused formation of prominent aggregates in almost 100% of dsRNA-treated cells (Figure 3B), and quantification analyses of the three evaluation parameters showed that CG6603 is the most potent suppressor of aggregates formation identified in our screen (Figure 2D), suggesting that it might play an important role in regulating the aggregation of mutant Htt protein. Because of this, we further examined its role during development and in neurodegeneration.

The CG6603 gene in Drosophila has not yet been extensively studied. Several mutant alleles of CG6603 exist, all of which cause early lethality when homozygous. By mosaic clonal analyses, we further found that patches of CG6603 mutant tissue failed to develop, indicating that the gene encodes an essential cellular function (data not shown). Further, overexpression of wild-type CG6603 caused a toxicity effect in the targeted tissues (Figure S3). Together, these results indicate that an optimal level of CG6603 activity is essential for normal animal development.

To study the role of CG6603 in neurodegeneration, we next tested its genetic interaction with HD93 (*Httex1p-93Q*), a well-characterized Drosophila HD model (Steffan *et al.* 2001). In HD93 flies, a mutant Htt containing a polyQ tract of 93 residues is ectopically expressed in the Drosophila eye, causing an age-dependent degeneration. At day 7, the degeneration is manifested exteriorly by the clear depigmentation in the posterior region of the eye (compare Figure 5B with 5A); as the fly ages this degeneration gradually spreads to the whole eye (compare Figure 5E with 5B). When tested in HD93 flies, CG6603 showed a strong dosage-dependent modifying effect on neurodegeneration: in flies heterozygous for mutations in CG6603, which halved the endogenous dosage of the corresponding protein, eye degeneration was significantly accelerated (Figure 5C). Furthermore, increasing the endogenous level of wild-type CG6603 by ectopically expressing low levels of CG6603 notably suppressed eye degeneration in HD93 flies (Figure 5F; see Figure S4 for additional controls for this assay).

CG6603 encodes a protein of 804 amino acids with significant sequence homology to the Hsp110 subfamily of chaperones, which is distinguished from other Hsp70 family chaperones by its unusually large size (Easton *et al.* 2000). Currently, alleles of CG6603 are referred to as Hsc70Cb, solely due to its cytological location at polytene band 70C. To avoid confusion with the general Hsp70 proteins, we refer to it as dHsp110 in this study. Consistent with our result that Hsp110 was the most potent suppressor of aggregates formation by mutant Htt, a previous study showed that mammalian Hsp110 conferred cellular thermo-resistance in cultured cells and was severalfold more efficient than Hsc70 in preventing aggregation of denatured luciferase (Oh *et al.* 1997). Thus, together with the observation of its dosage-dependentgenetic interaction with HD flies, Hsp110, a strong aggregation suppressor, might also be a potent suppressor of mutant polyQ-induced neurodegeneration.

***tra1* modulates the toxicity of mutant Htt *in vivo*:** In addition to *dhsp110*, we found that two mutant alleles of *tra1* (also called *Nipped-A*), another aggregation suppressor identified from the screen, also showed a dosage-dependent modifying effect on neurotoxicity of mutant Htt: in a heterozygous *tra1* mutant background, the eye degeneration of HD93 flies was significantly enhanced (Figure 5D), suggesting a role of *tra1* in mutant Htt-induced neurotoxicity. Similar to *hsp110*, knockdown of *tra1* significantly increased aggregates formation in the assay. *tra1* is believed to function in the Spt-Ada-Gcn5-Acetyltransferase complex to regulate transcription. It encodes a large protein containing a HEAT domain, a PI-3,4 kinase-like domain, and a TPR repeat. The role of *tra1* in regulating aggregates formation remains to be clarified.

DISCUSSION

A genomewide RNAi screen for regulators of aggregates formation in Drosophila cells: In Drosophila, which has been extensively used to study polyQ and other neurodegenerative diseases, most of the previous studies focused on toxicity; no systematic analysis of regulators of aggregates formation has been carried out in this system. By developing a cell-based quantitative assay and using a genomewide collection of dsRNAs in Drosophila, we performed a high-throughput RNAi screen and identified >100 aggregation regulators. Clearly, more studies are needed to further validate the identified candidates and investigate the exact mechanisms by which these regulators modulate aggregation. Nevertheless, this genomewide RNAi screen should help complement the previous studies focusing on toxicity in neurodegenerative diseases. For example, by comparing hits from our screen with previously identified toxicity modifiers in Drosophila, we found an interesting overlap between these two groups of genes. In addition, we showed that Drosophila *hsp110* (*CG6603*) and *tra1* can modify neurodegeneration of HD flies in a dosage-dependent manner. Together, these findings support that modulating aggregates formation might have therapeutical implications in treating neurodegenerative diseases.

Hsp110 chaperone as a potent suppressor of aggregates formation and neurotoxicity: From the screen, *hsp110* (CG6603) stands out as the most potent suppressor of aggregates formation. By further charac-

terizing its mutant phenotypes, we found that an optimal level of CG6603 activity is essential for normal animal development because both loss of its endogenous function and its high-level overexpression were detrimental to the animal. Moreover, CG6603 modulates neurodegeneration of HD flies in a dosage-dependent manner. Together, these data suggest a unique role for CG6603 in regulating normal animal development, protein folding, and neurotoxicity.

Notably, in COS-7 cells, overexpression of the Hsp110 family member Hsp105α suppresses both the aggregation and the cellular toxicity of the mutated androgen receptor, the causative gene for the polyQ disease spinalbulbar muscular atrophy (Ishihara *et al.* 2003). In addition, a Hsp110 homolog in *C. elegans* has recently been identified as a strong suppressor of aggregates formation by the ALS-associated mutant SOD1 (see below), and more interestingly, in a mouse ALS model, three Hsp110 family members were found to be physically associated with mutant but not wild-type SOD1 as animals age (Wang *et al.* 2009a,b). Together, these results suggest a conserved role of Hsp110 family chaperones in modulating misfolding and toxicity of mutant disease proteins.

Despite being highly conserved from yeast to humans, being one of the most abundant proteins in the mammalian brain and much more effective than Hsc70 in preventing aggregation of denatured protein, there are only limited functional studies on the Hsp110 family of proteins, and their exact biochemical function remains unclear (Oh *et al.* 1997, 1999; Easton *et al.* 2000; Shaner *et al.* 2005; Yam *et al.* 2005). It has been suggested that Hsp110 cannot on its own refold a denatured protein, but instead functions as a "holdase" by binding and maintaining the denatured protein in a soluble folding-competent state and subsequently cooperating with other Hsp70 chaperones for refolding (Oh *et al.* 1997, 1999; Shaner *et al.* 2005; Yam *et al.* 2005). More recently, Hsp110 proteins were also suggested as acting as nucleotide exchange factors for general Hsp70 chaperones (Dragovic *et al.* 2006; Raviol *et al.* 2006; Polier *et al.* 2008; Schuermann *et al.* 2008). Interestingly, although multiple families of chaperone proteins exist in eukaryotes, Hsp110 showed the strongest effect as an aggregates suppressor in the screen (Figure 2D and Figure 3B and data not shown). Chaperones function in diverse cellular processes, but each chaperone has a selective substrate preference (Bukau *et al.* 2006). In addition, chaperones display specificity in modulating polyQ neurotoxicity (Chan *et al.* 2000). Thus, given the dosage-sensitive effect of Hsp110 in normal Drosophila development and in modulating Htt toxicity, it is possible that Hsp110 plays a rate-limiting regulatory role for general Hsp70 chaperones, a role similar to that of Hsp40, which acts as a co-chaperone for Hsp70 chaperones by stimulating their ATPase activity (Craig *et al.* 1994; Bukau *et al.* 2006). Alternatively, Hsp110 might be the main chaperone that is more specific for the proper folding of mutant polyQ proteins. The detailed mechanism of action of Hsp110 proteins remains to be clarified. Nevertheless, results from our RNAi screen and genetic analyses, together with previous studies, suggest that Hsp110 chaperones play an important role in regulating the proper folding and toxicity of mutant Htt.

Comparison with aggregation regulators isolated from other large-scale RNAi screens in model organisms: Recently, several large-scale RNAi-based screens in *C. elegans* for aggregation regulators of different ND-associated proteins have been reported. We thus compared our candidates with those isolated from these studies.

A total of 186 suppressors were isolated from a genomewide RNAi screen for genes regulating polyQ aggregation in *C. elegans*, and knockdown of these genes by dsRNA promotes aggregates formation in muscles expressed a threshold-length polyQ protein (Q35-YFP) (Nollen *et al.* 2004). Comparison of the results of these two screens reveals many overlapping hits, including *hsf*, *Hsc70-5*, *uba1*, *T-cp1*, and *rab1*, as detailed in Table S3.

However, we also noted significant differences between the results of the two screens. For example, on one hand, knockdown of the *rme-8* gene, a DnaJ domain chaperone protein, could enhance aggregates formation in *C. elegans*, whereas its closest homolog in Drosophila, *Rme-8*, showed no effect in our study. On the other hand, the fly *dhdj1* gene (also called *hsp40 and dnaj1*), which encodes a DnaJ domain protein of the Hsp40 co-chaperone family, showed a strong effect in our study (Figure 3C) whereas its closest homolog in the worm, *dnaj-13*, was not found in the *C. elegans* study. In addition, many regulators from our study, such as *hsp110*, *JNK* members, and the *NMD* pathway, were not identified in the *C. elegans* screen, and vice versa. Most intriguingly, there are many cases where the same group of genes isolated from these two screens elicits different responses in the two systems, such as *rab1* and *Tbp-1*, as downregulation of these genes' expression led to an increased aggregates formation in the *C. elegans* study but to an opposite effect in our study (Table S3). Among such genes, perhaps the most obvious examples are those involved in protein biogenesis. In the *C. elegans* screen, 40 identified suppressors were ribosomal proteins, and their depletion by RNAi promoted premature formation of aggregates in the muscle (Nollen *et al.* 2004). In our study, 97 cytoplasmic and mitochondrial ribosomal proteins were also isolated from the primary screen. However, knockdown of these ribosomal proteins in the assay significantly diminished aggregates formation in Drosophila cells (see Table S3, Figure S2, and File S1). Because formation of aggregates is sensitive to the level of Htt mutant expression (Scherzinger *et al.* 1999), and ribosomal proteins are involved in general protein synthesis, we suspect that the effect of these ribosomal proteins in our assay is likely to be indirect and thus removed from the follow-up studies.

The reason(s) behind the differences between these two screens is still not clear, but likely due to many factors, such as an intrinsic species difference between the fly and the worm, different assay approaches (visual inspection of whole animals *vs.* computer imaging of cultured cells), or differential sensitivity of the experimental system (muscle tissue in *C. elegans vs.* Drosophila S2 cell lines). However, one important element might be that, compared with the cell-based assay that reflects mainly an autonomous cellular effect, *C. elegans* as a complicated multi-cellular organism can integrate the sensing and responses to the aggregates-induced stress within a specific tissue (*e.g.*, the muscle) at the whole-animal level, eliciting both autonomous and more complicated nonautonomous responses (Prahlad and Morimoto 2009). Indeed, one recent study suggested that thermosensory neurons regulate the cellular heat-shock response in *C. elegans* (Prahlad *et al.* 2008). Further investigations will be needed to address these different observations. Nevertheless, hits from these two screens should complement each other because they provide a valuable comparison that can broaden our understanding of the regulation of aggregates formation in different experimental systems.

A major component of the Lewy bodies inclusions in Parkinson's disease is α-synuclein (α-Syn) (Spillantini *et al.* 1997). In two similar RNAi screens in *C. elegans*, one genomewide and the other targeting 868 candidates, 84 and 20 hits, respectively, were identified. When knocked down, these hits increased aggregation of fluorescence-tagged human α-Syn expressed in worm body-wall muscles (Hamamichi *et al.* 2008; van Ham *et al.* 2008). Comparison of our result with these two studies revealed only limited overlaps: in both cases, a chaperone protein—Hsp83 or Dnaj-1 (Hsp40), respectively (Table S4 and Table S5).

Mutations in the human superoxide dismutase (SOD1) gene are associated with ALS (Rosen *et al.* 1993; Bruijn *et al.* 2004; Pasinelli and Brown 2006). A whole-genome RNAi screen in *C. elegans* identified 81 suppressors, which, when knocked down by RNAi increased aggregates formation in neurons expressing the YFP-tagged misfolding-prone SOD1 (G85R) mutant (Wang *et al.* 2009a). Interestingly, homologs of eight of these hits were also identified in our study, including *hsf*, *hsp110*, and *rab11*, with another four among the candidates from our primary screen (Table S6). Again we noted several cases where two homologous genes elicited opposite responses in the two screens (*e.g.*, *uba2* and *rab11*; see Table S6). We hypothesize that, as in the above polyQ study, similar factors might be accountable for such opposite responses in this SOD1 screen as well. Nevertheless, the observation of more overlapping hits among polyQ, Htt (a polyQ disease gene), and SOD1 mutants than with α-Syn raises an intriguing possibility that polyQ and SOD1 mutants share more similarities in their aggregation processes than with α-Syn.

Note: While the manuscript for this study was being prepared, a RNAi screen similar to this study was reported by Doumanis *et al.* (J. Doumanis, K. Wada, Y. Kino, A. W. Moore and N. Nukina, 2009, RNAi screening in Drosophila cells identifies new modifiers of mutant Huntingtin aggregation. PLoS One **4:** e7275) who used a Httex1-62Q-eGFP reporter in Drosophila BG2 cells and identified 21 regulators after testing 7200 Drosophila genes. Comparing the results from the two screens revealed several similarities (Table S7). First, 3 identical genes were isolated from both screens: *sec23*, *deflated* (*defl*), and *CG4738* (Table S7). Importantly, these 3 genes showed similar effects on aggregation in both screens: knocking down of *sec23* and *CG4378* decreased aggregates formation, while reducing the level of *defl* increased aggregates formation. In addition, another 6 genes from the Doumanis *et al.* (2009) study were among the original 644 candidates from our primary screens, which were eventually removed from our final hit list after failing to pass the second screens. These 6 genes also showed similar effects on aggregates formation in both studies (Table S7). Moreover, we noted that, although Nup154, one of the hits from the Doumanis *et al.* (2009) study, was not identified in our screen, several other Nup family proteins, including Nup62, Nup98, Nup170, and Nup 358, were isolated from our screen. The remaining differences between the results of the two studies are likely due to different selection criteria as well as different RNAi libraries and cell types used in the screens. It is highly likely that, due to unavoidable variations in the experiments, extra false positives are included and extra false negatives are removed from both studies. Additional analyses are warranted to examine the identified regulators from these studies. Nevertheless, the significant overlap of the hits from these two independent screens supports the reproducibility of the image-based RNAi screen for studying regulations of aggregates formation. Further experiments will be needed to validate the *in vivo* effects of the identified candidates from these screens and uncover the mechanisms underlying their regulations.

We thank the Hereditary Disease Foundation (HDF) for providing mutant Htt plasmids; L. Thompson, J. L. Marsh, N. Bonini, and M. Feany for providing advice and Drosophila stocks; the Drosophila RNAi Screening Center for providing technical support; B. Mathey-Prevot for advice and critical reading of the manuscript; M. Markstein and R. Griffin for critical reading of the manuscript; members of the Perrimon lab for assistance, in particular J. Phillips and P. Bradley for microscopy and image analysis; and C. Villalta for fly injection. R.Z. is a Fellow of the Leukemia and Lymphoma Society; S.Z. gratefully acknowledges support in the form of a fellowship from the Harvard Center for Neurodegeneration and Repair as well as the Lieberman Award from the HDF. N.P. is an Investigator of the Howard Hughes Medical Institute.

LITERATURE CITED

Andrew, S. E., Y. P. Goldberg, B. Kremer, H. Telenius, J. Theilmann *et al.*, 1993 The relationship between trinucleotide (CAG) re-

peat length and clinical features of Huntington's disease. Nat. Genet. **4:** 398–403.

Arrasate, M., S. Mitra, E. S. Schweitzer, M. R. Segal and S. Finkbeiner, 2004 Inclusion body formation reduces levels of mutant huntingtin and the risk of neuronal death. Nature **431:** 805–810.

Bilen, J., and N. M. Bonini, 2005 Drosophila as a model for human neurodegenerative disease. Annu. Rev. Genet. **39:** 153–171.

Boutros, M., A. A. Kiger, S. Armknecht, K. Kerr, M. Hild *et al.*, 2004 Genome-wide RNAi analysis of growth and viability in Drosophila cells. Science **303:** 832–835.

Brand, A. H., and N. Perrimon, 1993 Targeted gene expression as a means of altering cell fates and generating dominant phenotypes. Development **118:** 401–415.

Bruijn, L. I., T. M. Miller and D. W. Cleveland, 2004 Unraveling the mechanisms involved in motor neuron degeneration in ALS. Annu. Rev. Neurosci. **27:** 723–749.

Bukau, B., J. Weissman and A. Horwich, 2006 Molecular chaperones and protein quality control. Cell **125:** 443–451.

Caplen, N. J., J. Fleenor, A. Fire and R. A. Morgan, 2000 dsRNA-mediated gene silencing in cultured Drosophila cells: a tissue culture model for the analysis of RNA interference. Gene **252:** 95–105.

Caughey, B., and P. T. Lansbury, 2003 Protofibrils, pores, fibrils, and neurodegeneration: separating the responsible protein aggregates from the innocent bystanders. Annu. Rev. Neurosci. **26:** 267–298.

Chan, H. Y., J. M. Warrick, G. L. Gray-Board, H. L. Paulson and N. M. Bonini, 2000 Mechanisms of chaperone suppression of polyglutamine disease: selectivity, synergy and modulation of protein solubility in Drosophila. Hum. Mol. Genet. **9:** 2811–2820.

Chan, H. Y., J. M. Warrick, I. Andriola, D. Merry and N. M. Bonini, 2002 Genetic modulation of polyglutamine toxicity by protein conjugation pathways in Drosophila. Hum. Mol. Genet. **11:** 2895–2904.

Chang, H. C., S. L. Newmyer, M. J. Hull, M. Ebersold, S. L. Schmid *et al.*, 2002 Hsc70 is required for endocytosis and clathrin function in Drosophila. J. Cell Biol. **159:** 477–487.

Chang, H. C., M. Hull and I. Mellman, 2004 The J-domain protein Rme-8 interacts with Hsc70 to control clathrin-dependent endocytosis in Drosophila. J. Cell Biol. **164:** 1055–1064.

Chen, H. K., P. Fernandez-Funez, S. F. Acevedo, Y. C. Lam, M. D. Kaytor *et al.*, 2003 Interaction of Akt-phosphorylated ataxin-1 with 14–3–3 mediates neurodegeneration in spinocerebellar ataxia type 1. Cell **113:** 457–468.

Clemens, J. C., C. A. Worby, N. Simonson-Leff, M. Muda, T. Maehama *et al.*, 2000 Use of double-stranded RNA interference in Drosophila cell lines to dissect signal transduction pathways. Proc. Natl. Acad. Sci. USA **97:** 6499–6503.

Cooper, A. A., A. D. Gitler, A. Cashikar, C. M. Haynes, K. J. Hill *et al.*, 2006 Alpha-synuclein blocks ER-Golgi traffic and Rab1 rescues neuron loss in Parkinson's models. Science **313:** 324–328.

Craig, E. A., J. S. Weissman and A. L. Horwich, 1994 Heat shock proteins and molecular chaperones: mediators of protein conformation and turnover in the cell. Cell **78:** 365–372.

Doumanis, J., K. Wada, Y. Kino, A. W. Moore and N. Nukina, 2009 RNAi screening in Drosophila cells identifies new modifiers of mutant Huntingtin aggregation. PLoS One **4:** e7275.

Dragovic, Z., S. A. Broadley, Y. Shomura, A. Bracher and F. U. Hartl, 2006 Molecular chaperones of the Hsp110 family act as nucleotide exchange factors of Hsp70s. EMBO J. **25:** 2519–2528.

Easton, D. P., Y. Kaneko and J. R. Subjeck, 2000 The hsp110 and Grp1 70 stress proteins: newly recognized relatives of the Hsp70s. Cell Stress Chaperones **5:** 276–290.

Fernandez-Funez, P., M. L. Nino-Rosales, B. de Gouyon, W. C. She, J. M. Luchak *et al.*, 2000 Identification of genes that modify ataxin-1-induced neurodegeneration. Nature **408:** 101–106.

Franceschini, N., 1972 Pupil and pseudopupil in the compound eye of Drosophila, pp. 75–82 in *Information Processing in the Visual Sysytem of Arthropods*, edited by R. Wehner. Springer-Verlag, Berlin.

Friedman, A., and N. Perrimon, 2007 Genetic screening for signal transduction in the era of network biology. Cell **128:** 225–231.

Garcia-Mata, R., Z. Bebok, E. J. Sorscher and E. S. Sztul, 1999 Characterization and dynamics of aggresome formation by a cytosolic GFP-chimera. J. Cell Biol. **146:** 1239–1254.

Gatfield, D., L. Unterholzner, F. D. Ciccarelli, P. Bork and E. Izaurralde, 2003 Nonsense-mediated mRNA decay in Drosophila: at the intersection of the yeast and mammalian pathways. EMBO J. **22:** 3960–3970.

Gusella, J., and M. MacDonald, 2002 No post-genetics era in human disease research. Nat. Rev. Genet. **3:** 72–79.

Hamamichi, S., R. N. Rivas, A. L. Knight, S. Cao, K. A. Caldwell *et al.*, 2008 Hypothesis-based RNAi screening identifies neuroprotective genes in a Parkinson's disease model. Proc. Natl. Acad. Sci. USA **105:** 728–733.

Huntington's Disease Collaborative Research Group, 1993 A novel gene containing a trinucleotide repeat that is expanded and unstable on Huntington's disease chromosomes. Cell **72:** 971–983.

Ishihara, K., N. Yamagishi, Y. Saito, H. Adachi, Y. Kobayashi *et al.*, 2003 Hsp105alpha suppresses the aggregation of truncated androgen receptor with expanded CAG repeats and cell toxicity. J. Biol. Chem. **278:** 25143–25150.

Kanuka, H., E. Kuranaga, T. Hiratou, T. Igaki, B. Nelson *et al.*, 2003 Cytosol-endoplasmic reticulum interplay by Sec61alpha translocon in polyglutamine-mediated neurotoxicity in Drosophila. Proc. Natl. Acad. Sci. USA **100:** 11723–11728.

Kazantsev, A., E. Preisinger, A. Dranovsky, D. Goldgaber and D. Housman, 1999 Insoluble detergent-resistant aggregates form between pathological and nonpathological lengths of polyglutamine in mammalian cells. Proc. Natl. Acad. Sci. USA **96:** 11404–11409.

Kazemi-Esfarjani, P., and S. Benzer, 2000 Genetic suppression of polyglutamine toxicity in Drosophila. Science **287:** 1837–1840.

Kulkarni, M. M., M. Booker, S. J. Silver, A. Friedman, P. Hong *et al.*, 2006 Evidence of off-target effects associated with long dsRNAs in Drosophila melanogaster cell-based assays. Nat. Methods **3:** 833–838.

Ma, Y., A. Creanga, L. Lum and P. A. Beachy, 2006 Prevalence of off-target effects in Drosophila RNA interference screens. Nature **443:** 359–363.

Marhold, J., I. Torok, I. Iliopoulos, A. Mishra, C. De Lorenzo *et al.*, 2000 The TPR-containing Spaghetti protein interacts with Hsp90 and is required for cell survival and differentiation in imaginal discs. 41st Annual Drosophila Research Conference, Pittsburgh, PA **41:** 616c.

Marsh, J. L., and L. M. Thompson, 2006 Drosophila in the study of neurodegenerative disease. Neuron **52:** 169–178.

Morimoto, R. I., 2008 Proteotoxic stress and inducible chaperone networks in neurodegenerative disease and aging. Genes Dev. **22:** 1427–1438.

Nollen, E. A., S. M. Garcia, G. van Haaften, S. Kim, A. Chavez *et al.*, 2004 Genome-wide RNA interference screen identifies previously undescribed regulators of polyglutamine aggregation. Proc. Natl. Acad. Sci. USA **101:** 6403–6408.

Oh, H. J., X. Chen and J. R. Subjeck, 1997 Hsp110 protects heat-denatured proteins and confers cellular thermoresistance. J Biol. Chem. **272:** 31636–31640.

Oh, H. J., D. Easton, M. Murawski, Y. Kaneko and J. R. Subjeck, 1999 The chaperoning activity of hsp110. Identification of functional domains by use of targeted deletions. J. Biol. Chem. **274:** 15712–15718.

Pasinelli, P., and R. H. Brown, 2006 Molecular biology of amyotrophic lateral sclerosis: insights from genetics. Nat. Rev. Neurosci. **7:** 710–723.

Penney, J. B., Jr., J. P. Vonsattel, M. E. MacDonald, J. F. Gusella and R. H. Myers, 1997 CAG repeat number governs the development rate of pathology in Huntington's disease. Ann. Neurol. **41:** 689–692.

Polier, S., Z. Dragovic, F. U. Hartl and A. Bracher, 2008 Structural basis for the cooperation of Hsp70 and Hsp110 chaperones in protein folding. Cell **133:** 1068–1079.

Prahlad, V., and R. I. Morimoto, 2009 Integrating the stress response: lessons for neurodegenerative diseases from C. elegans. Trends Cell Biol. **19:** 52–61.

Prahlad, V., T. Cornelius and R. I. Morimoto, 2008 Regulation of the cellular heat shock response in Caenorhabditis elegans by thermosensory neurons. Science **320:** 811–814.

Ravikumar, B., C. Vacher, Z. Berger, J. E. Davies, S. Luo *et al.*, 2004 Inhibition of mTOR induces autophagy and reduces tox-

icity of polyglutamine expansions in fly and mouse models of Huntington disease. Nat. Genet. **36:** 585–595.

Raviol, H., H. Sadlish, F. Rodriguez, M. P. Mayer and B. Bukau, 2006 Chaperone network in the yeast cytosol: Hsp110 is revealed as an Hsp70 nucleotide exchange factor. EMBO J. **25:** 2510–2518.

Rosen, D. R., T. Siddique, D. Patterson, D. A. Figlewicz, P. Sapp *et al.*, 1993 Mutations in Cu/Zn superoxide dismutase gene are associated with familial amyotrophic lateral sclerosis. Nature **362:** 59–62.

Ross, C. A., and M. A. Poirier, 2005 Opinion: What is the role of protein aggregation in neurodegeneration? Nat. Rev. Mol. Cell Biol. **6:** 891–898.

Rubin, G. M., M. D. Yandell, J. R. Wortman, G. L. Gabor Miklos, C. R. Nelson *et al.*, 2000 Comparative genomics of the eukaryotes. Science **287:** 2204–2215.

Scherzinger, E., R. Lurz, M. Turmaine, L. Mangiarini, B. Hollenbach *et al.*, 1997 Huntingtin-encoded polyglutamine expansions form amyloid-like protein aggregates in vitro and in vivo. Cell **90:** 549–558.

Scherzinger, E., A. Sittler, K. Schweiger, V. Heiser, R. Lurz *et al.*, 1999 Self-assembly of polyglutamine-containing huntingtin fragments into amyloid-like fibrils: implications for Huntington's disease pathology. Proc. Natl. Acad. Sci. USA **96:** 4604–4609.

Schuermann, J. P., J. Jiang, J. Cuellar, O. Llorca, L. Wang *et al.*, 2008 Structure of the Hsp 110:Hsc70 nucleotide exchange machine. Mol. Cell **31:** 232–243.

Shaner, L., H. Wegele, J. Buchner and K. A. Morano, 2005 The yeast Hsp110 Sse1 functionally interacts with the Hsp70 chaperones Ssa and Ssb. J. Biol. Chem. **280:** 41262–41269.

Shulman, J. M., and M. B. Feany, 2003 Genetic modifiers of tauopathy in Drosophila. Genetics **165:** 1233–1242.

Sisodia, S. S., 1998 Nuclear inclusions in glutamine repeat disorders: Are they pernicious, coincidental, or beneficial? Cell **95:** 1–4.

Snell, R. G., J. C. MacMillan, J. P. Cheadle, I. Fenton, L. P. Lazarou *et al.*, 1993 Relationship between trinucleotide repeat expansion and phenotypic variation in Huntington's disease. Nat. Genet. **4:** 393–397.

Spillantini, M. G., M. L. Schmidt, V. M. Lee, J. Q. Trojanowski, R. Jakes *et al.*, 1997 Alpha-synuclein in Lewy bodies. Nature **388:** 839–840.

Steffan, J. S., L. Bodai, J. Pallos, M. Poelman, A. McCampbell *et al.*, 2001 Histone deacetylase inhibitors arrest polyglutamine-dependent neurodegeneration in Drosophila. Nature **413:** 739–743.

Steffan, J. S., N. Agrawal, J. Pallos, E. Rockabrand, L. C. Trotman *et al.*, 2004 SUMO modification of Huntingtin and Huntington's disease pathology. Science **304:** 100–104.

Valencia-Sanchez, M. A., and L. E. Maquat, 2004 An enemy within: fly reconnaissance deploys an endonuclease to destroy nonsense-containing mRNA. Trends Cell Biol. **14:** 594–597.

van Ham, T. J., K. L. Thijssen, R. Breitling, R. M. Hofstra, R. H. Plasterk *et al.*, 2008 C. elegans model identifies genetic modifiers of alpha-synuclein inclusion formation during aging. PLoS Genet. **4:** e1000027.

Wang, J., G. W. Farr, D. H. Hall, F. Li, K. Furtak *et al.*, 2009a An ALS-linked mutant SOD1 produces a locomotor defect associated with aggregation and synaptic dysfunction when expressed in neurons of Caenorhabditis elegans. PLoS Genet. **5:** e1000350.

Wang, J., G. W. Farr, C. J. Zeiss, D. J. Rodriguez-Gil, J. H. Wilson *et al.*, 2009b Progressive aggregation despite chaperone associations of a mutant SOD1-YFP in transgenic mice that develop ALS. Proc. Natl. Acad. Sci. USA **106:** 1392–1397.

Warrick, J. M., H. Y. Chan, G. L. Gray-Board, Y. Chai, H. L. Paulson *et al.*, 1999 Suppression of polyglutamine-mediated neurodegeneration in Drosophila by the molecular chaperone HSP70. Nat. Genet. **23:** 425–428.

Weston, C. R., and R. J. Davis, 2002 The JNK signal transduction pathway. Curr. Opin. Genet. Dev. **12:** 14–21.

Whitesell, L., and S. L. Lindquist, 2005 HSP90 and the chaperoning of cancer. Nat. Rev. Cancer **5:** 761–772.

Wu, C., Z. Fayazi, S. Marion, X. Bao, M. Shero *et al.*, 2005 2005 Modulation of polyglutamine toxicity and aggregation by dMLF and its interaction with 14–3–3zeta and dMADM. 46th Annual Drosophila Research Conference, San Diego, CA **46:** 923B.

Yam, A. Y., V. Albanese, H. T. Lin and J. Frydman, 2005 Hsp110 cooperates with different cytosolic HSP70 systems in a pathway for de novo folding. J. Biol. Chem. **280:** 41252–41261.

Communicating editor: O. Hobert

GENETICS

Supporting Information
http://www.genetics.org/cgi/content/full/genetics.109.112516/DC1

A Genomewide RNA Interference Screen for Modifiers of Aggregates Formation by Mutant Huntingtin in Drosophila

Sheng Zhang, Richard Binari, Rui Zhou and Norbert Perrimon

DOI: 10.1534/genetics.109.112516

FILE S1

Materials and Methods

Plasmid constructs

DNA fragments containing the mutant Httex1-Qn-eGFP variants (Q25, Q46, Q72 and Q103) were cloned from DNA constructs generously provided by the Hereditary Disease Foundation (HDF) (originally from Dr. A. Kazantsev (KAZANTSEV *et al*. 1999)). To clone into the hygromycin-resistance pMK33 vector which contains the copper-inducible *metallothionein* promoter, the Httex1-Q25-eGFP and Httex1-Q103-eGFP fragments were digested with XhoI and SpeI restriction enzymes and inserted into the same sites in the pMK33 vector, while the Httex1-Q46-eGFP as well as Httex1-Q72-eGFP were amplified by PCR and inserted blunt-ended into EcoRV site in the pMK33 vector.

For generating transgenic flies, DNA containing the Httex1-Q25-eGFP and Httex1-Q103-eGFP fragments were digested with XhoI and XbaI and inserted into the same sites in the pUAST vector (BRAND and PERRIMON 1993), and DNA containing the Httex1-Q46-eGFP and Httex1-Q72-eGFP fragments were digested with KpnI and SpeI and inserted into the same sites in the pUAST vector.

A cDNA encoding CG6603 (the fly Hsp110) was obtained from the Berkeley *Drosophila* Genome Project (clone ID LD32979). The EcoRI/XhoI fragment containing full-length CG6603 was cloned into the EcoRI and XhoI sites of pUAST vector.

Cell culture

Drosophila SL2 cells (Schneider's Line S2 cells; http://www.flyrnai.org) were grown at 25°C in Schneider's media (GIBCO) with 5% heat inactivated fetal bovine serum (FBS; JRH Biosciences). Each of the mutant Httex1-Qn-eGFP constructs in pMK33 vector was transfected into SL2 cells using Effectene reagents (QIAGEN) and selected with 0.2mg/ml of Hygromycin consecutively for 5 generations to establish stably-transformed SL2 lines. The resulting stable cell lines are maintained in Hygromycin-containing medium.

Secondary screens

To eliminate genes that could indirectly affect aggregates formation, the 644 candidate genes from the primary screen were further evaluated and tested using the following criteria (Figs. 2E , S2 and their legends for more details): (1) *Remove dsRNAs with significant off-target effects:* we removed candidates with dsRNA amplicons that contain 21-bp overlaps with more than 5 other genes in the genome, as knockdown of the expression of these overlapping genes would be expected to cause a significant non-specific off-target RNAi effects (KULKARNI *et al.* 2006; MA *et al.* 2006). (http://www.flyrnai.org/); (2) *Remove candidates that function in general protein synthesis*: we studied the available information about the known functions of the candidate genes isolated from the primary screen, mainly through checking the references in Flybase (http://flybase.bio.indiana.edu/) and the PubMed in NCBI (National Center for Biotechnology Information) (http://www.ncbi.nlm.nih.gov/). From these analyses, we found that a large number of genes are involved in general protein synthesis, including 97 genes encoding cytoplasmic or mitochondrial ribosomal proteins. Knockdown of all these genes in the assay significantly reduced aggregates formation, but since the formation of aggregates depends upon the amount of available mis-folded Htt protein (SCHERZINGER *et al*. 1999), it is highly likely that the observed reduction is not specific to aggregates formation, but simply reflects a general decrease in overall protein synthesis within the cell. Accordingly, most of these ribosomal proteins were not pursued in the following validation steps. (3) *Re-test the dsRNAs from the primary screen*: to ensure the reproducibility of the effects of these candidate dsRNAs on aggregates formation, we performed an intermediate screen by re-synthesizing and re-testing the amplicons specific to genes

retained from the primary screen up to this point. More specifically, DNA templates for the dsRNA amplicons used in the primary screen were re-amplified, and the corresponding dsRNAs were re-synthesized and re-tested for 8 additional rounds. Candidates that failed to repeat their effect on modulating aggregation in these additional rounds of testing were removed; (4) *Luciferase assay*: since the expression of the Httex1-Q46-eGFP reporter in the screen was controlled by the inducible *metallothionein* promoter, genes that regulate the activity of this promoter would also be identified in the primary and intermediate screens. To eliminate such promoter-related false positives, we established stable cell lines in which the expression of luciferase was controlled by the same *metallothionein* promoter, and performed luciferase-based assays to examine the effect of candidate dsRNAs on the activity of the *metallothionein* promoter (see below). Using this luciferase-based secondary assay, we eliminated a number of candidates that affect cellular copper uptake or the activity of the *metallothionein* promoter in the pMK33 vector, which controls the expression of the Httex1-Qp46 reporter (*e.g.,* COP complex components). (5) *Validation with 2nd set of dsRNAs*: to further ensure that the modulating effect observed in the primary screen was specific only for the candidate genes, for each candidate that passed the above selections, one or two more sets of dsRNAs targeting different regions of this candidate gene were synthesized and re-tested. Genes that failed to repeat their effect on modulating aggregation in these additional rounds of testing were removed from consideration.

As with the primary screen, 384-well plates were used in all the secondary assays, with 5ul of 50ng/ul dsRNA samples or water controls aliquoted into each well in the plate. As different to the primary screen, in each secondary assay plate, more than 100 evenly-positioned wells were aliquoted with 5ul of water as controls. For all the secondary assays, the effect of dsRNA treatment on aggregates formation was evaluated on the same three evaluation parameters (*i.e.,* the average number, size and intensity of the aggregates), but instead of using the values from the whole plate as an evaluation standards, average values and standard deviation (SD) from these more than 100 water control wells were used as evaluation standards for each plate. Accordingly, in the secondary assays, those dsRNAs that decreased or increased aggregates formation by more than 2xSD of the water controls on the plate were considered to have a significant effect on aggregates formation and were selected as hits.

126 hits passed all the above selection steps. Table S2 provides details regarding the amplicons used in this study, and additional information is available at the DRSC website (http://www.flyrnai.org).

Luciferase-based assay on the *metallothionein* promoter

Two stable cell lines (RZ-1 and RZ-14) were generated, each carrying three transgenes encoding the Firefly luciferase, Renilla luciferase and a hairpin (a *Renilla luciferase* hairpin in RZ-14, a *firefly luciferase* hairpin in RZ-1), all under the control of the *metallothionein* promoter. About 20,000 cells were treated with ~200 ng dsRNA in 384-well plates and induced with 25 uM $CuSO_4$ 72 hours after dsRNA treatment. Luciferase assay was performed after another 48 hours following the manufacture's recommendation (Promega). The firefly luciferase activity (in RZ-14) and the *Renilla* luciferase activity (in RZ-1) were employed to access the effect of dsRNA treatment on the *metallothionein* promoter activity.

***Drosophila* stocks and genetic crosses**

pUAST-dHsp110 (CG6603) DNA and pUAST-Httex1-Qn-eGFP DNA were injected into *w1118* embryos and transformants were selected following standard procedures. Around 20 independent transgenic lines for each of the constructs were established and tested. Targeted expression of Httex1-Qn-eGFP (Q25, Q46, Q72 and Q103) or dHsp110 (CG6603) was achieved using the binary UAS-Gal4 expression system (BRAND and PERRIMON 1993). A *gmr-Gal4* driver was used for all eye-specific expression (HAY *et al*. 1994).

Although CG6603 encodes the only Hsp110 ortholog in *Drosophila*, alleles of CG6603 refer to it as Hsc70Cb, solely due to its cytological location at polytene band 70C. To avoid confusion with the general Hsp70 proteins, we renamed it it as dHsp110. The following mutant alleles for *Drosophila dhsp110* (CG6603) were tested: *l(3)70Ca*^{1} (From the Bloomington Stock Center, stock # BL-4911), *l(3)00082* (BL-11485), *l(3)S148513* (from the Szeged *Drosophila* Stock Centre at University of Szeged, stock

010975), *l(3)S004112* (stock # 0100040), *l(3)S031820* (stock # 0100228), *l(3)S064906* (stock # 0100467), and *l(3)S0134802* (stock # 0100866). The following *dhsp110* alleles showed dosage-dependent genetic interaction with the HD93 flies: *l(3)00082*, *l(3)S031820, l(3)S064906, l(3)S004112* and *l(3)S0134802*. To test for genetic interactions, HD93 flies (Httex1p-Q93, genotype *gmr-Gal4/+; UAS-Httex1p-Q93*. from Drs. L. Thompson and J.L. Marsh (STEFFAN *et al*. 2001)) were crossed to the above *dhsp110* mutant alleles or the *UAS*-dHsp110 transformants, and *w1118* or *UAS*-LacZ transgenic flies were used as cross controls. The resulting trans-heterozygous progeny were collected and aged for the same time as the progeny from the *w1118* and *UAS*-LacZ control crosses (genotype for the mutant *dhsp110* crosses: *gmr-Gal4/+; UAS-Httex1p-Q93/+; dhsp110*$^{-}$/+; genotype for the *UAS*-dHsp110 cross: *gmr-Gal4/+; UAS-Httex1p-Q93 /+; UAS-dHsp110*/+; genotype for the *w1118* control: *w1118; gmr-Gal4/+; UAS-Httex1p-Q93*/+. genotype for the *UAS*-LacZ control: *gmr-Gal4/+; UAS-Httex1p-Q93/+; UAS-LacZ*/+). Eye imaging was done using a Zeiss Stemi SV11 microscope. To generate mosaic mutant clones, three *dhsp110* alleles, *l(3)00082, l(3)S031820* and *l(3)S064906,* were recombined onto an FRT80B chromosome, and mosaic mutant clones in adults were generated according to standard procedures using the *eyeless*-Flipase and *hs*-Flipase drivers *(XU and RUBIN 1993)*. In the eye, mosaic clones homozygous for either of the three *dhsp110* alleles were not viable.

REFERENCES

BRAND, A. H., and N. PERRIMON, 1993 Targeted gene expression as a means of altering cell fates and generating dominant phenotypes. Development **118:** 401-415.

HAY, B. A., T. WOLFF and G. M. RUBIN, 1994 Expression of baculovirus P35 prevents cell death in Drosophila. Development **120:** 2121-2129.

KAZANTSEV, A., E. PREISINGER, A. DRANOVSKY, D. GOLDGABER and D. HOUSMAN, 1999 Insoluble detergent-resistant aggregates form between pathological and nonpathological lengths of polyglutamine in mammalian cells. Proc Natl Acad Sci U S A **96:** 11404-11409.

KULKARNI, M. M., M. BOOKER, S. J. SILVER, A. FRIEDMAN, P. HONG *et al*., 2006 Evidence of off-target effects associated with long dsRNAs in Drosophila melanogaster cell-based assays. Nat Methods **3:** 833-838.

MA, Y., A. CREANGA, L. LUM and P. A. BEACHY, 2006 Prevalence of off-target effects in Drosophila RNA interference screens. Nature **443:** 359-363.

SCHERZINGER, E., A. SITTLER, K. SCHWEIGER, V. HEISER, R. LURZ *et al*., 1999 Self-assembly of polyglutamine-containing huntingtin fragments into amyloid-like fibrils: implications for Huntington's disease pathology. Proc Natl Acad Sci U S A **96:** 4604-4609.

STEFFAN, J. S., L. BODAI, J. PALLOS, M. POELMAN, A. MCCAMPBELL *et al*., 2001 Histone deacetylase inhibitors arrest polyglutamine-dependent neurodegeneration in Drosophila. Nature **413:** 739-743.

XU, T., and G. M. RUBIN, 1993 Analysis of genetic mosaics in developing and adult Drosophila tissues. Development **117:** 1223-1237.

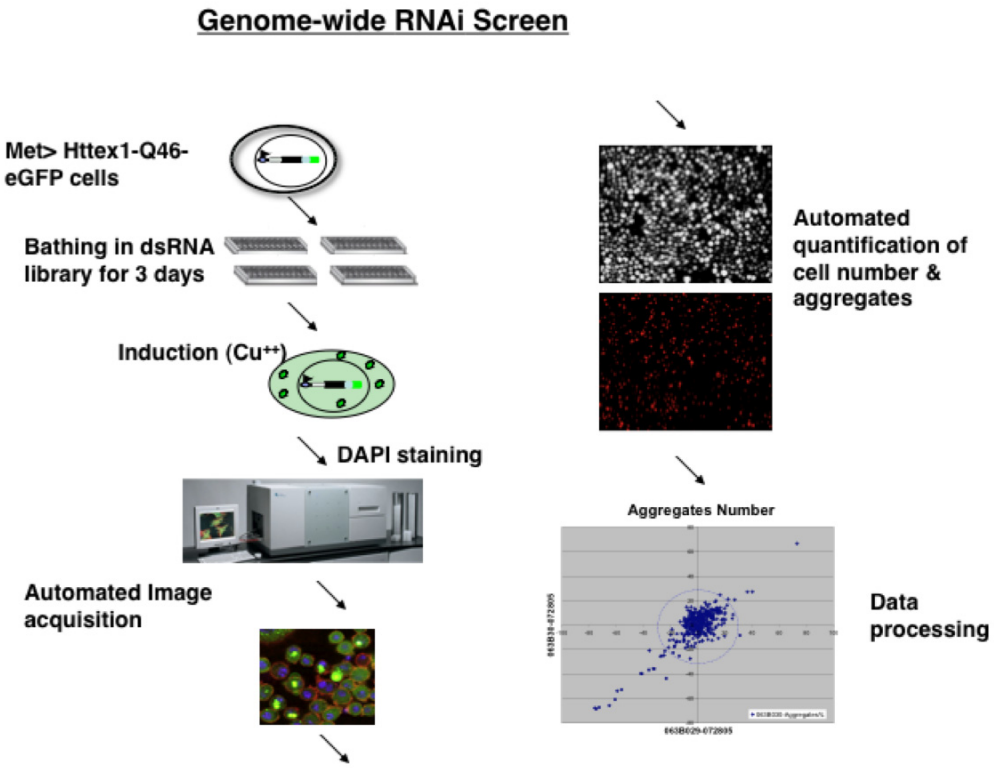

FIGURE S1.—Procedure for genome-wide RNAi screen on aggregation modulators. Httex1-Qp46 cells were mixed with the dsRNAs in 384-well plates for 3 days to knock down target gene expression. Copper ($CuSO_4$) was then added to induce reporter expression and aggregates formation, and after two days, the cells were fixed and stained with DAPI and Tritc-labeled phalloidin to reveal the cell nuclei and overall cell morphology, respectively. Images, from four sites in each well (equal to about 4,000 cells), were then collected to identify the eGFP aggregates. Information on both the aggregates and cell number in the imaged fields were automatically quantified using the Metamorph analytic software (Fig. 2C, also see Materials and Methods for details). This method allowed us to accurately quantify the effect of dsRNA treatment on the average number, size and intensity of aggregates, which were normalized with cell numbers. For each plate, the average value and standard deviation (SD) for these three parameters from the whole plate samples were also calculated. In the primary screen, for a dsRNA-treated sample, if the value of any of the three parameters was beyond 2xSD of the whole plate average, it was considered to have a significant effect on aggregates formation and was selected as a potential candidate.

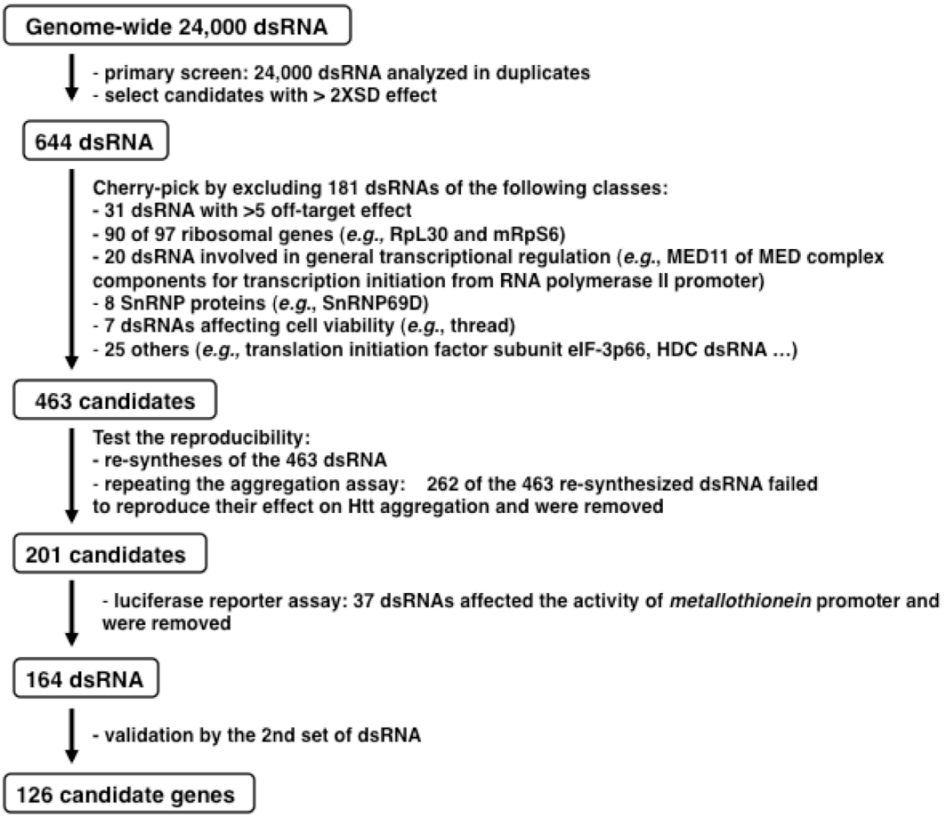

FIGURE S2.—Flow chart of the RNAi screening and validation steps for aggregation modulators of mutant Htt. In primary screen, genome-wide *Drosophila* RNAi libraries containing >24,000 dsRNA were tested in duplicates and 644 dsRNA with significant effect (over 2XSD of a plate average) on aggregates formation were isolated (see Fig. S1 and "Secondary screens" below for details).

Out of these 644 dsRNA, sequences of 31 dsRNA turned out to have high off-target effect (targeting over five different genes) and were removed from the ensuing studies. Curation of the remaining corresponding genes' known functions revealed that many are involved in general protein synthesis, including 97 ribosomal proteins, 8 SnRNP proteins, components of transcription initiation complexes and translation initiation factors. 131 of such dsRNA were also excluded from further analyses.

Amplicons for the remaining 463 dsRNA were cherry-picked and their dsRNA were re-synthesized and re-tested in the same aggregation assay. 262 of the re-synthesized dsRNA failed in the repeating experiments while the other 201 dsRNA showed reproducible effect.

In a luciferase-based assay to identify false positives that act by regulating the activity of the *metallothionein* promoter employed in the aggregation assay, 37 of the above 201 dsRNA showed significant effect, including those involved in general transcriptional regulation or cellular endocytosis (*e.g.*, Cop complex components such as alpha-COP, beta-Cop and zeta-Cop). These 37 dsRNA were excluded from further consideration.

Lastly, to confirm the specificity of the dsRNA with their corresponding genes, one or two more set of dsRNA targeting different regions of the remaining 164 candidates were synthesized and re-tested. In total, 126 genes passed all these validation steps.

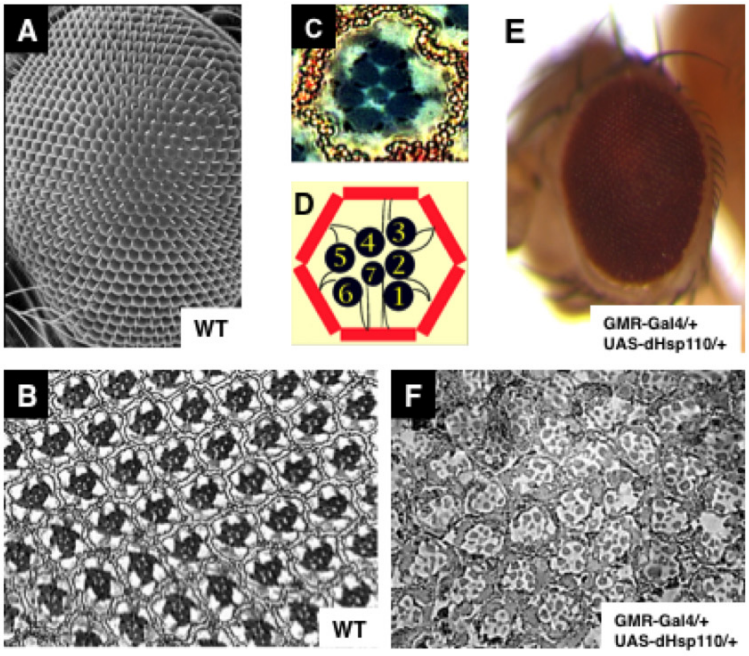

FIGURE S3.—High level of *dhsp110* (*CG6603*) expression disrupts the proper formation of adult *Drosophila* eye.

(A-D) Wild-type (wt) adult flies have well-patterned eye structure. (A) A wt adult eye imaged by scanning electronic microscopy. Each eye is composed of about 800 ommatidia. (B) Well-organized internal structure of adult eye, which is composed of lattice-like ommatidium units as revealed by tangential section. (C and D) (C) High magnification view of a single ommatidium unit and (D) its cartoon representation. Each ommatidium is composed of 8 photoreceptor cells (PR) surrounded by pigment cells. Only 7 PR cells are visible in each sectioned layer. (E and F) Images of adult fly eyes with high-level *dhsp110* expression. Genotype: *GMR-Gal4/+; UAS-dhsp110/+*. Although these flies show normal external eye morphology (E, bright-field imaging), their internal eye structure are severely disrupted (F, tangential section image), including a thickening of pigment cells, loss of PR cells and abnormally formed rhabdomeres.

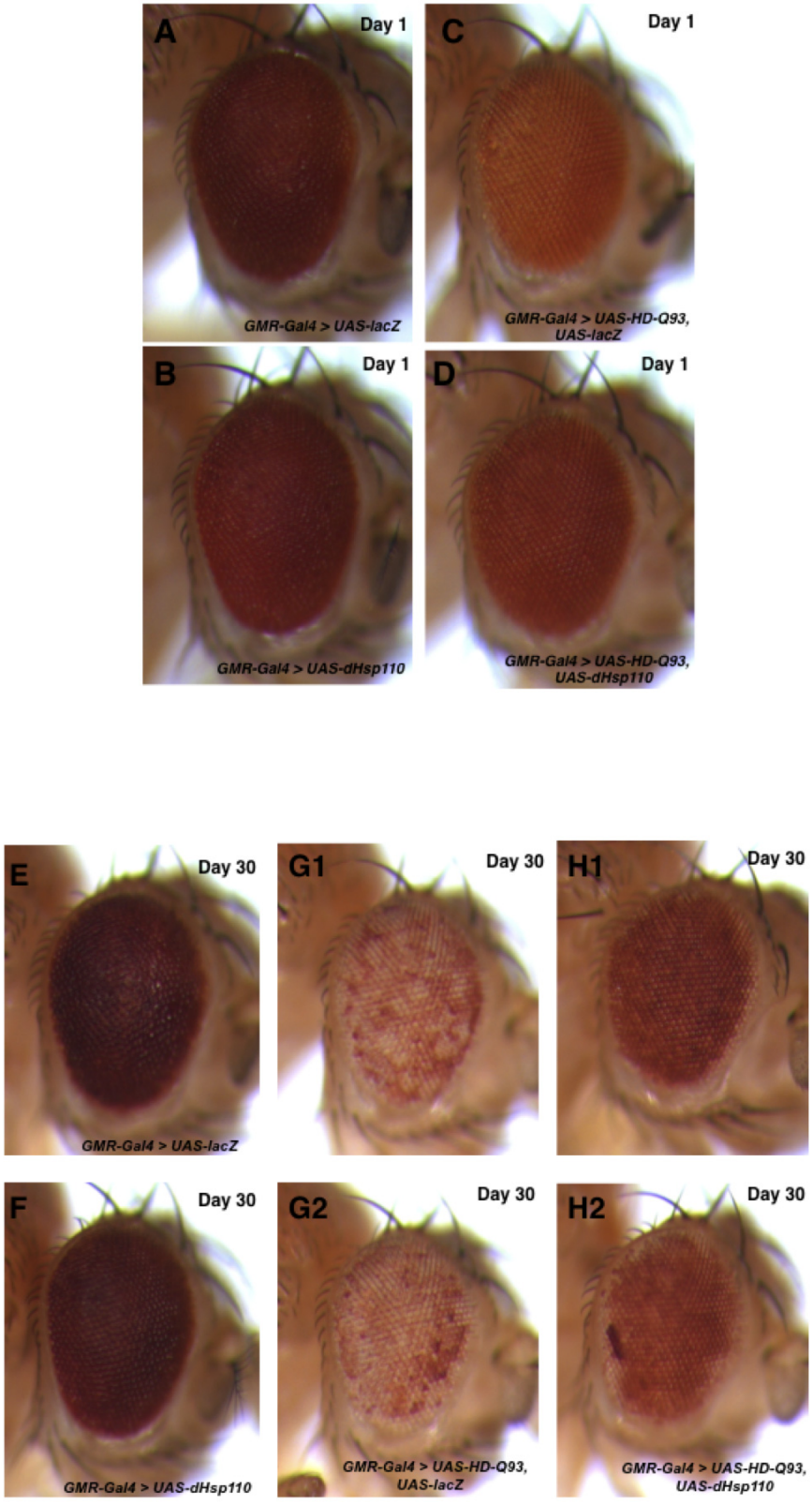

FIGURE S4.—Modification of HD93 toxicity by *dhsp110*. Bright-filed images of adult fly eyes at age (A-D) day 1 or (E-H) day 30. Control flies that express (A and E) lacZ gene or (B and F) dhsp110 alone did not show obvious loss of pigmentation as

flies age. Flies that co-express *Httex1p-Q93* with (C, G1 and G2) lacZ gene show a clear de-pigmentation of adult eyes as they age, (D, H1 and H2) while such degeneration phenotype was significantly suppressed by the presence of *dhsp110* gene. Genotypes: (A and E) *GMR-Gal4/+; UAS-LacZ/+*. (B and F) *GMR-Gal4/+; UAS-dhsp110/+*. (C, G1 and G2) *GMR-Gal4/ UAS-LacZ; UAS-Httex1p Q93/+*. (D, H1 and H2) *GMR-Gal4/ UAS-dhsp110; UAS-Httex1p Q93* /+ (STEFFAN *et al*. 2001). In all eye images, the anterior side is up and the ventral side is to the left.

Tables S1-S7 are available for download as Excel files at http://www.genetics.org/cgi/content/full/genetics.109.112516/DC1

TABLE S1

List of hits identified from the RNAi screen as regulators of aggregates formation

Please note that in this study, "**Suppressor**" is defined genetically as the candidates that cause an increased formation of aggregates after dsRNA-mediated knockdown of the corresponding genes, whereas "**Enhancer**" is similarly defined as those that cause a decreased formation of aggregates in the assay.

The columns in the Table S1 are as follows: (1) Gene symbol; (2) Modifier class "Enhancer" and "Suppressor".; (3) Functional categorization (based on the "GeneOntology (GO)" index biological function or protein domains.); (4) IDs of DRSC amplicons (http://www.flyrnai.org/); (5) FBGN: ID of FlyBase Genome annotations; (6) Protein domain (from the Flybase: http://flybase.bio.indiana.edu/); (7) Molecular function (curated from the Flybase)

TABLE S2

List of hits identified from the RNAi screen as regulators of aggregates formation and their human homologues

The columns in the Table S2 are as follows: (1) Gene symbol; (2) Gene full name; (3) Functional categorization (based on the "GeneOntology (GO)" index biological function or protein domains); (4) Modifier class (see Table S1 for definition of "Enhancer" and "Suppressor"); (5) Gene ID by CG number (http://flybase.bio.indiana.edu/) (6) Human homologues by "Database of Pairwise Orthologs" (http://inparanoid.cgb.ki.se/); (7) Human homologues (curated from the Homophila website http://superfly.ucsd.edu/homophila); (8) Disease-related human orthologs (curated from the Homophila website http://superfly.ucsd.edu/homophila).

TABLES S3-S7

Notes

1. Please note that for consistence, the effects of the *C. elegans* modifiers and their *Drosophila* homologues on aggregates formation are described according to Nollen et. al., (2004) as "*Enhance*" or "*Suppress*", respectively. "Enhance" indicates that the cognate dsRNA treatment increases aggregation formation, and *vise versa*, "Suppress" suggests that the cognate dsRNA treatment reduces aggregation formation.

2. **Importantly**, in our study and in Table S1 and S2, the identified modifiers are listed as "***Suppressor***" and "***Enhancer***". "Suppressor" is defined *genetically* as the genes for which their cognate dsRNA treatment enhances aggregation formation, that is, causing an increased formation of aggregates after dsRNA-mediated knockdown of the corresponding genes, whereas "Enhancer" is similarly defined as those that lead to a decreased formation of aggregates in the assay. Accordingly, genes that cause "Enhance" and "Suppress" effect in Tables S3-S6 correspond to the "Suppressor" and "Enhancer" in our study as listed in Tables S1 and S2, respectively.

3. In Tables S3-S6, information on the *C. elegans* modifiers are directly from the corresponding studies. *Drosophila* homologues (column E) of the *C. elegans* genes were identified manually by first downloading the protein sequences of the worm modifiers from the NCBI website with the "cosmid nr." or other information listed in respective studies, which were then used to search the *Drosophila* database (**http://flybase.bio.indiana.edu/**) using the BLASTp program from the NCBI site. In most cases, only the closet homologues were listed and compared with the hits from our study.

4. *Drosophila* homologues that were also identified in the primary screens in our study are labeled as "1st", those identified as final candidates after passing all the secondary assays are marked as "F".

TABLE S3

Comparison of modifiers from this study in Drosophila and the Nollen *et. al.,* study (2004) in *C. elegans*

Drosophila homologues that were also identified in our primary screens are labeled in column G as "1st", those identified as final candidates after passing all the secondary assays are marked in column H as "F. The effects of the *C. elegans* modifiers and their *Drosophila* homologues on aggregates formation are listed in column C and F, respectively (See the above **Notes** for more details).

The protein sequences for the worm modifiers were retrieved using the "cosmid nr." listed in Nollen et. al., (2004) study. "**-**" in column E indicates that no *Drosophila* homologue of the corresponding worm gene was identified from the search. Protein sequences for a few worm modifiers could not be retrieved from the NCBI website using the "cosmid nr." provided and were indicated as "none" in column E.

TABLE S4

Comparison of modifiers for mutant Htt aggregation from this study in Drosophila and for mutant *a-Synuclein* by the Hamamichi *et al.* study in *C. elegans* (2008)

The effects of the genes on aggregates formation in corresponding assays are listed in columns C and G, respectively. Please see "**Notes**" in front of the Table S3 for more details.

* For *dnj-19*, a DnaJ domain co-chaperone, its closest homologue in *Drosophila* is *droj2* (FBGN0038145) with E value at 4.79546e-47. *dnaJ-1* (FBgn0015657), another homolog of this gene (E value of 1.63364e-20), marked in column H as "1st" and in column I as "F", was the only overlapping hit from these two studies

TABLE S5

Comparison of modifiers for mutant Htt aggregation from this study in *Drosophila* and for mutant *α-Synuclein* by the *van Ham et al.* study in *C. elegans* (2008)

Information on the *C. elegans* modifiers are directly from the Table 1 and Table S1 in the *van Ham et al*. (2008) study**.** Please see "**Notes**" in front of the Table S3 for more details.

The protein sequences of the worm modifiers were downloaded from the NCBI website with the "*Cosmid no*." or "Gene" provided in Table 1 and Table S1 in *van Ham et al*. (2008) study. **"-"** in column E indicates that no *Drosophila* homologues was identified from the search. Protein sequences for a few worm modifiers could not be retrieved from the NCBI website using the "*Cosmid no*." or "Gene" provided in Table 1 and Table S1 in *van Ham et al*. (2009) study and were indicated with "**?**".

The five *Drosophila* homologues that were isolated in the primary screens from our study are labeled in column H as "1st".

* For chaperone *R151.7*, its closest *Drosophila* homolog is *trap1* (FBgn0026761) with E value at 2.73574e-150. *hsp83* (FBgn0001233), another homolog of this gene (E value of 1.06342e-42), was also isolated as a final candidate in our study and is marked as "F" in column I.

TABLE S6

Comparison of modifiers for mutant Htt aggregation from this study in *Drosophila* and for mutant SOD from the Wang *et. al.,* study (2009) in *C. elegans*

Drosophila homologues that were identified in the primary screens from our study are labeled in column H as "1st", those isolated as final candidates are marked as "F" in column I. Please see "**Notes**" in front of the Table S3 for more details.

"-" in column E indicates that no *Drosophila* homologue of the corresponding worm gene was identified.

"*" For *dnj-19*, a DnaJ domain co-chaperone, its closest homolog in *Drosophila* is *droj2* (FBgn0038145) with E value at 4.79546e-47. Its homology with *dnaJ-1* (FBgn0015657) is at a E value of 1.63364e-20.

TABLE S7

Comparison of modifiers from Doumanis *et. al.,* study (2009) with the candidates from this study

Please see "**Notes**" in front of the Table S3 for more details. The same modifiers that were also identified in our primary screens are labeled in column D as "1st", those identified as final candidates after passing all the secondary assays are marked in column F as "F".